TGF- induces oncofetal fibronectin, which in turn modulates TGF- superfamily signaling in endothelial cells

Ventura, Elisa ; Weller, Michael ; Macnair, Will ; Eschbach, Katja ; Beisel, Christian ; Cordazzo, Cinzia ; Claassen, Manfred ; Zardi, Luciano ; Burghardt, Isabel

Abstract: Gene splicing profiles are frequently altered in cancer, and the splice variants of fibronectin (FN) that contain the extra-domains A (EDA) or B (EDB), referred to as EDA+FN or EDB+FN, are highly upregulated in tumor vasculature. Transforming growth factor (TGF-) signaling has been attributed a pivotal role in glioblastoma, with TGF- promoting angiogenesis and vessel remodeling. By using immunohistochemistry staining, we observed that the oncofetal FN isoforms EDA+FN and EDB+FN are expressed in glioblastoma vasculature. single-cell gene expression profiling of tumors by using CD31 and -smooth muscle actin (SMA) as markers for endothelial cells, and pericytes and vascular smooth muscle cells (VSMCs), respectively, confirmed the predominant expression of FN, EDA+FN and EDB+FN in the vascular compartment of glioblastoma. Specifically, within the CD31-positive cell population, we identified a positive correlation between the expression of EDA+FN and EDB+FN, and of molecules associated with TGF- signaling. Further, TGF- induced EDA+FN and EDB+FN in human cerebral microvascular endothelial cells and glioblastoma-derived endothelial cells in a SMAD3- and SMAD4-dependent manner. In turn, we found that FN modulated TGF- superfamily signaling in endothelial cells via the EDA and EDB, pointing towards a bidirectional influence of oncofetal FN and TGF- superfamily signaling.

DOI: https://doi.org/10.1242/jcs.209619

TGF-β induces oncofetal fibronectin, which in turn modulates TGF-β superfamily signaling in endothelial cells

Elisa Ventura[1], Michael Weller[1], Will Macnair[2], Katja Eschbach[3], Christian Beisel[3], Cinzia Cordazzo[4], Manfred Claassen[2], Luciano Zardi[4], Isabel Burghardt[1].

[1]Laboratory of Molecular Neuro-Oncology, Department of Neurology, University Hospital and University of Zurich, Frauenklinikstrasse 26, 8091 Zurich, Switzerland.
[2]Institute of Molecular Systems Biology, ETH Zurich, Zurich, Switzerland.
[3]Department of Biosystems Science and Engineering, ETH Zürich, 4058 Basel, Switzerland.
[4]Sirius-biotech, c/o Advanced Biotechnology Center, Genoa, Italy.

Corresponding author: Isabel Burghardt
Tel.: 0041 (0) 44 2551967
Fax: 0041 (0) 044 2554507
E-Mail: isabel.burghardt@usz.ch

Key words: TGF-β, EDA+FN, EDB+FN, glioblastoma

JCS Advance Online Article. Posted on 20 November 2017

SUMMARY STATEMENT

Oncofetal fibronectin expression positively correlates with the expression of TGF-β and TGF-β-related molecules in glioblastoma blood vessels. In endothelial cells TGF-β induces oncofetal fibronectin, in turn modulating TGF-β superfamily signaling.

ABSTRACT

Gene splicing profiles are frequently altered in cancer, and the splice variants of fibronectin (FN) containing the extra-domains A (EDA) and B (EDB) referred to as EDA+FN and EDB+FN are highly up-regulated in tumor vasculature. TGF-β signaling has been attributed a pivotal role in glioblastoma, with TGF-β promoting angiogenesis and vessel remodeling. By immunohistochemical staining, we observed that the oncofetal FN isoforms EDA+FN and EDB+FN are expressed in glioblastoma vasculature. *Ex vivo* single cell gene expression profiling of patients' tumors using the markers CD31 and alpha-smooth muscle actin (αSMA) respectively confirmed the predominant expression of FN, EDA+FN, and EDB+FN in the vascular compartment of glioblastoma. Specifically, within the CD31-positive cell population, we identified a trend of positive correlation in the expression of EDA+FN and EDB+FN with molecules associated with TGF-β signaling. Further, TGF-β induced EDA+FN and EDB+FN in human cerebral microvascular endothelial cells and glioblastoma-derived endothelial cells in a SMAD3/SMAD4-dependent manner. In turn, FN modulated TGF-β superfamily signaling in endothelial cells via the EDA and EDB domains, pointing towards a bidirectional influence between oncofetal FN and TGF-β superfamily signaling.

INTRODUCTION

Fibronectins (FN) are high molecular mass adhesive glycoproteins of the extracellular matrix (ECM) involved in several processes including cell growth and differentiation, cell adhesion and migration (Hynes, 1990; Pankov and Yamada, 2002). FN is encoded by a single gene (Zardi et al., 1982), but various isoforms are generated by alternative splicing mechanisms and post-translational modifications (Schwarzbauer, 1991). Three FN regions can be affected by alternative splicing: the extra-domain A (EDA), the extra-domain B (EDB) and the type III connecting sequence (IIICS) (Pankov and Yamada, 2002; Schwarzbauer, 1991). Specifically, the EDA and EDB domains may be included or excluded by exon usage or skipping (Pankov and Yamada, 2002). Both the EDA- and EDB-containing isoforms, EDA+FN and EDB+FN, preferentially appear in neo-vessels during embryogenesis and physiological angiogenesis as well as in pathological conditions including wound healing, atherosclerosis and tumorigenesis (Carnemolla et al., 1989; Castellani et al., 1994; Ffrench-Constant et al., 1989; Rybak et al., 2007; Zardi et al., 1987). Therefore EDA+FN and EDB+FN are also termed oncofetal FN isoforms. EDB+FN is expressed around vasculature exclusively during neo-angiogenesis (Castellani et al., 1994) so that antibodies specific for EDB+FN injected in tumor-bearing mice or cancer patients specifically accumulate in the tumor vasculature (Neri and Bicknell, 2005; Santimaria et al., 2003). The EDB-specific antibody L19 is presently under investigation in clinical trials in cancer patients as one moiety of fusion proteins with cytokines such as interleukin-2 (NCT02957019) (Carnemolla et al., 2002; Zegers et al., 2015) or tumor necrosis factor (TNF)-α (NCT02076620) (Borsi et al., 2003; Danielli et al., 2015), or radio-labeled (Borsi et al., 2002; Erba et al., 2012; Poli et al., 2013).

Several genetic studies ascribed a fundamental role of FN in the morphogenesis and physiology of blood vessels (Astrof and Hynes, 2009). Transforming growth factor (TGF)-β superfamily members are fundamental regulators of endothelial cell physiology, too (Pardali and ten Dijke, 2009). The TGF-β superfamily consists of 33 members, including the three TGF-β isoforms, TGF-β1, TGF-β2 and TGF-β3, and ten bone morphogenetic proteins (BMP). TGF-β superfamily signaling is triggered by the binding of TGF-β superfamily ligands to two functional classes of transmembrane receptors, known as type I, also known as the activin-like kinase (ALK), and type II receptors. Upon ligand binding, the type I/II TGF-β receptor heterocomplex is formed

and type I receptors, in turn, phosphorylate the receptor-regulated SMAD (R-SMAD) proteins. The phosphorylated R-SMAD together with the co-SMAD, SMAD4, translocate into the nucleus and modulate gene expression depending on the type and state of the cell (Massague, 2012). The type I receptors ALK4, ALK5 and ALK7 phosphorylate SMAD2 and 3, whereas ALK1,2,3 and 6 phosphorylate SMAD1,5 and 8. TGF-β signaling is commonly mediated by the ALK5/SMAD2/SMAD3 axis. However, in endothelial cells, TGF-β may also promote SMAD1,5,8 activation by the endothelium-specific receptor ALK1 (Goumans et al., 2002). Beyond, ALK5 has been shown to regulate SMAD1,5 signaling as well (Liu et al., 2009). Importantly, TGF-β responses also occur independently of SMAD through the activation of TGF-β-dependent non-canonical signaling pathways including the phospho-inositide 3' kinase (PI3K)/Akt pathway (Zhang et al., 2013), the mitogen-activated protein kinase MAPK/ERK pathway, and the p38 and c-Jun N-terminal kinase (JNK) pathways (Moustakas and Heldin, 2005).

Functional interactions between TGF-β and FN have been reported. TGF-β induces FN expression in different cell types (Ignotz and Massague, 1986). Also, TGF-β has been identified as one of the most important regulators of alternative splicing affecting the EDA and EDB of FN leading to an increase in EDA+FN and EDB+FN in several cell types (Balza et al., 1988; Borsi et al., 1990; Viedt et al., 1995). On the other hand, FN and its receptor integrin α5β1 positively regulate TGF-β- and BMP-induced SMAD1,5,8 phosphorylation by promoting the formation of a complex of ALK1 and the TGF-β superfamily co-receptor endoglin in human microvascular endothelial cells (Tian et al., 2012). Beyond, in fibroblasts, a role for EDA+FN in influencing TGF-β activity has been suggested (Muro et al., 2008; Serini et al., 1998; White et al., 2008).

TGF-β is a central regulator of the malignant phenotype of glioblastoma, the most common and aggressive malignant primary brain tumor of adults (Rodon et al., 2014; Wang et al., 2016). In glioblastoma, TGF-β has a central role in both inducing angiogenesis and promoting vessel remodeling (Dieterich et al., 2012). FN is up-regulated in glioblastoma vessels (Dieterich et al., 2012) with EDB+FN expression being abundant and positively correlating with tumor grade in gliomas (Castellani et al., 2002). Here we extend these investigations on FN in gliomas by investigating EDA+FN as well. We also aim at better understanding the interplay of glioma-derived oncogenic TGF-β and oncofetal FN at the tumor-vasculature interface.

RESULTS

Expression of EDA+FN and EDB+FN and of TGF-β signaling-associated molecules correlates in glioblastoma blood vessels.

We first investigated the expression of total FN and of the EDA+FN and EDB+FN isoforms in ten human glioblastoma sections and also stained non-tumor human brain tissues derived from four patients with epilepsy as controls. We used the antibodies IST-5, reacting with a FN domain common to all FN isoforms, IST-9, reacting with the EDA domain, and C6, specific for EDB+FN (Fig. 1A). In all sections investigated, tumor-associated vessels, identified by staining serial sections for the endothelial cell marker CD31, showed high levels of FN, EDA+FN and EDB+FN, whereas the tumor tissue itself was negative for EDA+FN and EDB+FN and showed only low or very low levels of total FN (Fig. 1B, representative sections of two glioblastoma patients are shown). In all non-tumor tissues analyzed, blood vessels were strongly positive for total FN, but negative or weakly positive for EDA+FN and negative for EDB+FN (Fig. 1B, representative sections of one patient with epilepsy are shown). Accordingly, mRNA analysis of freshly dissociated glioblastoma samples divided into CD31+ and CD31- fractions showed that FN, EDA+FN, and EDB+FN were preferentially expressed in the CD31+ fraction containing the endothelial cells (Fig. 1C). Pericytes and vascular smooth muscle cells (VSMC) express alpha-smooth muscle actin (αSMA) and αSMA expression is restricted to the tumor blood vessels in glioblastoma (Fig. 1D). Given the vascular distribution of FN, EDA+FN and EDB+FN in glioblastoma we asked whether pericytes/VSMC may also be involved in FN expression in glioblastoma. We therefore aimed at a more detailed expression analysis performing single cell real-time polymerase chain reaction (scRT-PCR) of FN, EDA+FN and EDB+FN and of CD31 and αSMA as markers of the endothelial and pericytic/VSMC cells respectively in cells derived from six different freshly dissociated human glioblastoma tissues. Of 465 single cells analyzed, 35 were selected as CD31-positive and 164 were selected as αSMA-positive (Fig. S1). Indeed, FN, EDA+FN, and EDB+FN were preferentially expressed in CD31+ *vs.* CD31- cells (Fig. 1E, upper panels) and in αSMA+ *vs.* αSMA- cells (Fig. 1E, lower panels), suggesting that both endothelial cells and perivascular cells contribute to the expression of EDA+FN and EDB+FN in glioblastoma blood vessels. With around half of the CD31+ cells also showing αSMA expression on mRNA levels (Fig. S1), we

also confirmed that endothelial cells may express αSMA in glioblastoma (Huang et al., 2016). In line, investigating CD31+ cells isolated from freshly dissociated tumor tissues from four other patients, we confirmed expression of αSMA in this *ex vivo* model. Since it has been reported that EDA+FN controls αSMA expression in fibroblasts (Serini et al., 1998), we performed selective gene silencing, reaching more than 90% in all models for both targets (data not shown), of EDA+FN or EDB+FN in four CD31+ cell lines derived from human glioblastoma tissue (ZH-464, ZH-483-2, ZH-613, ZH-616). EDA+FN and EDB+FN gene silencing reduced αSMA mRNA levels in all the four cell lines (Fig. 1F), suggesting a role for EDA+FN and EDB+FN in the regulation of αSMA expression in glioblastoma-derived endothelial cells.

Since TGF-β induces FN (Ignotz and Massague, 1986) and since alternative splicing of FN, including the generation of EDA+FN and EDB+FN, is mainly regulated by TGF-β in several cell types, we also considered the three TGF-β isoforms, TGF-β1, TGF-β2 and TGF-β3 in our single cell analysis of the six glioblastoma patients for a correlation analysis in the CD31+ and αSMA+ cell subpopulations. With regard to the CD31+ subpopulation, we observed a trend of positive correlation in the expression of TGF-β1 and FN (r^2=0.13, p=3.5e-02), TGF-β1 and EDA+FN (r^2=0.22, p=4.3e-03) and of TGF-β3 and FN (r^2=0.12, p=3.8e-02) and EDB+FN (r^2=0.14, p=2.5e-02) (Fig. 2, upper panels). In the αSMA+ cell fraction, all TGF-β isoforms showed a significant, but overall less pronounced positive correlation with the expression of FN, EDA+FN, and EDB+FN (Fig. 2, lower panels). Of note, in both CD31+ and αSMA+ cells, we also observed a positive correlation in the expression of FN and of transforming-growth factor β-induced (TGFBI) (Fig. 2), an extracellular matrix protein which is associated with malignancy and which is TGF-β-inducible (Gopal et al., 2017). Relevant proteins for TGF-β storage and activation in the ECM also include the latent TGF-β binding proteins (LTBP) with the isoforms LTBP1, LTBP2, LTBP3 and LTBP4 (Robertson et al., 2015). Therefore we also included these targets into the analysis which revealed a significant positive correlation of LTBP1 and FN, EDA+FN, and EDB+FN, of LTPB2 and FN and EDA+FN, and of LTBP3 and FN in the CD31+ cell fraction (Fig. 2, upper panels). All LTBP molecules significantly positively correlated with FN, EDA+FN, and EDB+FN in the αSMA+ cell fraction, except for LTBP3 and EDB+FN (Fig. 2, lower panels).

TGF-β1, TGF-β2 and TGF-β3 induce FN, EDA+FN, and EDB+FN in endothelial cells.

To investigate the potential regulation of EDA+FN and EDB+FN expression by TGF-β isoforms in endothelial cells *in vitro*, we used human cerebral microvascular endothelial cells (hCMEC). Exposure to TGF-β1, TGF-β2 or TGF-β3 increased mRNA expression of total FN, EDA+FN, and EDB+FN, as wells as protein levels of soluble FN, EDA+FN and EDB+FN as measured in the conditioned culture media of hCMEC cells (Fig. 3A). We also measured the levels of FN incorporated in the insoluble extracellular matrix and found that the levels of insoluble total FN and EDA+FN were increased whereas the levels of insoluble EDB+FN were not significantly changed upon TGF-β treatment, suggesting that the EDB+FN isoform is mainly released into solution (Fig. S2). To explore the molecular mechanism by which TGF-β isoforms induce FN expression in hCMEC, we first used the TGF-βRI-specific kinase activity inhibitor SD-208 (Uhl et al., 2004). SD-208 abolished the TGF-β1-, TGF-β2- and TGF-β3-mediated induction of FN, EDA+FN, and EDB+FN on both mRNA and protein level (Fig. 3A), indicating that the process is TGF-βRI-dependent and equally valid for all three TGF-β isoforms. To further specify the signal transduction pathway downstream of the TGF-β receptors, we first investigated the canonical, SMAD-dependent TGF-β signaling pathway. Gene silencing of SMAD4, with an efficacy on mRNA level of ~88% (data not shown), inhibited the TGF-β1- and TGF-β2-induced increase in FN, EDA+FN, and EDB+FN on mRNA and protein levels, indicating the involvement of the SMAD signaling pathway (Fig. 3B, data for TGF-β1 not shown). Also, gene silencing of SMAD3, but not of SMAD2 (Fig. 3C, left panel), abolished the TGF-β1- and TGF-β2-dependent induction of FN, EDA+FN and EDB+FN expression (Fig. 3C, data for TGF-β1 not shown). The efficacy of the gene silencing on mRNA level was ~90% and ~60% for SMAD2 and SMAD3, respectively, and SMAD2 and SMAD3 gene silencing was also verified on protein level at the time when the cells were treated with TGF-β (data not shown). Notably, gene silencing of SMAD3 reduced the relative fraction of FN molecules containing EDB by two-fold, whereas the relative fraction of FN molecules containing EDA remained unchanged (Fig. 3C, right panel), pointing towards a specific role for SMAD3 in the control of the splicing of the EDB domain. The inhibitory effect of SMAD3 gene silencing on TGF-β1- and TGF-β2-mediated induction of FN, EDA+FN and EDB+FN also translated into reduced protein levels (Fig. 3C, central panels, data for TGF-β1 not shown).

Since a role for JNK in the TGF-β-dependent induction of FN expression has been reported in human fibrosarcoma cells (Hocevar et al., 1999) and in light of the known cross-talk between canonical/SMAD-dependent and non-canonical/SMAD-independent TGF-β signaling pathways, we also explored the role for JNK in our model. The JNK-specific inhibitor SP600125 had only minor inhibitory effects on the TGF-β2-dependent induction of total FN or EDA+FN but abolished the TGF-β2-dependent induction of EDB+FN on mRNA and protein levels (Fig. S3). These data suggest JNK signaling as potential additional pathway controlling EDB+FN splicing in hCMEC cells.

To investigate this process in a model more closely reflecting the *in vivo* situation, we analyzed the effect of TGF-β1 and TGF-β2 on FN in human glioblastoma-derived CD31+ cells. TGF-β1 and TGF-β2 induced the expression of FN, EDA+FN and EDB+FN in the two patient-derived CD31+ cell lines ZH-459 (Fig. 4A) and ZH-613 (Fig. 4B). In line with our results for hCMEC (Fig. 3), TGF-β2-induced expression of FN, EDA+FN and EDB+FN was TGF-βRI- (Fig. 4C) and SMAD3/SMAD4-dependent (Fig. 4D). In CD31+ cells derived from another glioblastoma patient (ZH-616), TGF-β2 did not induce FN, EDA+FN, and EDB+FB, but gene silencing of SMAD3 and SMAD4 even reduced basal levels of EDA+FN and EDB+FN (Fig. 4E).

EDA+FN and EDB+FN modulate TGF-β superfamily signaling in hCMEC.

In endothelial cells, TGF-β may activate both the SMAD1,5,8- and SMAD2,3-dependent signal transduction pathways involving ALK1 and ALK5 respectively (Goumans et al., 2002). Further, FN and integrin α5β1 may control SMAD1,5,8 phosphorylation by promoting the formation of ALK1/endoglin complexes (Tian et al., 2012). To decipher the situation in hCMEC cells with very low levels of pSMAD2 in basal conditions, we first performed ALK1 and ALK5 gene silencing. ALK1 gene silencing affected neither the phosphorylation of SMAD1,5 nor that of SMAD2,3 in both basal conditions and upon TGF-β stimulation (Fig. S4A). Gene-specific silencing of ALK5 (Fig. S4A), treatment with the TGF-βRI-specific kinase activity inhibitor SD-208 (Fig. S4B) or gene-specific silencing of TGF-βRII (Fig. S4C) inhibited the TGF-β-induced increase in SMAD1,5 and SMAD2,3 phosphorylation levels and reduced basal pSMAD3 levels, without affecting basal pSMAD1,5 levels. This implies that in hCMEC TGF-β-induced SMAD1,2,3,5 phosphorylation is TGF-βRII- and ALK5-dependent and that endogenous TGF-β rather controls basal pSMAD3 levels,

whereas basal pSMAD1,5 levels may be controlled by other members of the TGF-β superfamily such as BMP. With these data in mind, we further investigated the potential control of TGF-β superfamily signaling by EDA+FN and EDB+FN in endothelial cells by performing transient gene silencing of EDA+FN and EDB+FN in hCMEC, with EDA specific-knockdown also affecting the levels of total FN pointing towards the presence of EDA in the majority of the FN molecules (Fig. 5A, left panel). The levels of pSMAD1,5 were reduced in both siEDA+FN and siEDB+FN gene-silenced cells. Cells with EDA+FN gene silencing showed also reduced levels of pSMAD3, whereas the levels of pSMAD2 were unaffected (Fig. 5A). To evaluate the mechanism of the reduction of pSMAD levels by EDA+FN and EDB+FN gene-silencing, we analyzed the levels of TGF-β1 in the conditioned media of the respective cells. We did not look at the levels of the other TGF-β isoforms since hCMEC show low levels of TGF-β2 and undetectable levels of TGF-β3 (data not shown). TGF-β1 is synthesized as a proprotein (pro-TGF-β1, 55 kDa) and its processing results in the generation of two molecules, the pro-domain known as latency associated peptide (LAP, 37 kDa) and mature TGF-β1 (12.5 kDa) (Constam, 2014). After pro-TGF-β processing, a covalent dimer of the LAP and a covalent dimer of mature TGF-β1 remain non-covalently associated forming the small latent complex (SLC, ~ 110 kDa). Both the SLC and the secreted unprocessed pro-TGF-β1 covalently bind via LAP to molecules belonging to the LTBP family forming the large latent complex (LLC, ~ 270 kDa). In siEDA+FN cells-derived and to a less pronounced extent also in siEDB+FN cells-derived conditioned media, analyzed by immunoblot under reducing conditions, the levels of pro-TGF-β1 as well as LAP and mature TGF-β1 were reduced (Fig. 5B, left panel; the conditioned media of hCMEC with the gene silencing of TGF-β1 are shown to identify the correct bands). The analysis of the same conditioned media under non-reducing conditions revealed that the reduction in TGF-β1 levels in the conditioned media of the siEDA+FN and siEDB+FN cells went along with a reduction in the levels of TGF-β1/LLC (Fig. 5B, central panel). We also analyzed the respective lysate in order to detect intracellular TGF-β1 levels and found that upon EDA+FN and EDB+FN gene silencing the intracellular levels of pro-TGFβ1 and LAP were unchanged (Fig. 5B, right panel). In agreement, the mRNA levels of TGF-β1 were not significantly changed in siEDA+FN or siEDB+FN cells when compared to control cells (data not shown). Taken together this analysis differentiating TGF-β1 levels in the lysates and supernatants suggests

that FN and oncofetal FN do not affect TGF-β1 protein secretion but rather control the levels of TGF-β1 available extracellularly. Since the gene silencing of EDA+FN also affected total levels of FN and EDB+FN levels (see Fig. 5A, left panel), we extended our analysis by a different approach to confirm the specific involvement of the EDA and EDB domains in the control of SMAD phosphorylation. This was based on the use of recombinant FN fragments including or excluding the EDA and EDB domains (Fig. 5C). Indeed, hCMEC treated with a recombinant FN fragment containing the EDB domain and adjacent FN type III domains 7, 8 and 9 (7-EDB-8-9) showed reduced levels of pSMAD1,5 compared with untreated cells or cells treated with the corresponding FN fragment lacking the EDB domain (7-8-9). The levels of pSMAD2 and 3 were unchanged (Fig. 5D). Treatment with the recombinant EDB domain alone (without the adjacent domains 7, 8 and 9) had only minor effects on the pSMAD1,5 levels, indicating the involvement of flanking domains in mediating the EDB effect. Compared to untreated cells or cells treated with the recombinant fragments including the two flanking EDA domains 11-12 and lacking EDA, hCMEC cells treated with the recombinant EDA domain alone showed decreased levels of pSMAD1,5 whereas the levels of pSMAD2 and pSMAD3 were unaffected. pSMAD1,5 levels were reduced in cells treated with the FN fragment 11-12 to a lesser extent than in cells treated with the EDA domain alone (Fig. 5D). Upon stimulation with recombinant TGF-β2, both the FN fragments 7-EDB-8-9 and EDA inhibited the increase in the phosphorylation of SMAD1,5 and, to a lesser extent, of SMAD2,3 when compared to untreated cells or cells treated with FN fragments lacking the EDA and EDB domains (Fig. 5E), confirming that both the EDA and the EDB domains of fibronectin are involved in the modulation of TGF-β superfamily signaling in hCMEC.

DISCUSSION

The FN splice isoforms containing the EDA and EDB domains, EDA+FN and EDB+FN, are strongly expressed in the vasculature and the heart of the developing embryo (Astrof and Hynes, 2009). After completion of developmental processes, both EDA+FN and EDB+FN are down-regulated and are almost undetectable in mature adult blood vessels and tissues, except in tissues undergoing physiological remodeling and angiogenesis, like the uterus and the ovary. During pathological tissue remodeling, in chronically inflamed tissues and tumors, these oncofetal FN isoforms are re-expressed and accumulate around newly forming vessels (Astrof and Hynes, 2009). In particular, EDB+FN is considered a marker of angiogenesis since its expression in the adult blood vasculature is restricted to vessels undergoing neo-angiogenesis (Castellani et al., 1994).

Previous reports showed that FN is up-regulated in glioblastoma vasculature (Dieterich et al., 2012) and that in gliomas the percentage of vessels expressing EDB+FN correlates with tumor grade (Castellani et al., 2002). Here we show that in glioblastoma the expression of not only the isoform EDB+FN, but also the isoform EDA+FN is abundant and restricted to tumor vasculature (Fig. 1B). In addition, we show that both CD31+ and αSMA+ cells derived from freshly dissociated glioblastoma, representing endothelial cells and pericytes/VSMC, respectively, express FN, EDA+FN, and EDB+FN showing the contribution of both endothelial and perivascular cells to the production of EDA+FN/EDB+FN in glioblastoma blood vessels (Fig. 1C,E). Fibroblasts, which are characterized by αSMA expression, are rare cells in the brain. However, a subpopulation of cells showing properties of cancer-associated fibroblasts, expressing αSMA and localizing around blood vessels, has been isolated in glioblastoma (Clavreul et al., 2012). Thus, there may be a minor contribution of αSMA+ cells derived from fibroblasts-like cells in addition to the one of pericytes/VSMC in expressing (oncofetal) FN. Overall, as shown in Fig. 1D and as previously reported (Takeuchi et al., 2010), αSMA shows a vascular distribution pattern in glioblastoma, so that the vast majority of the cells included in the αSMA+ cell subpopulation is blood vessel-associated. Endothelial cells in glioblastoma may undergo endothelial-to-mesenchymal transition (End-MT) and express αSMA (Huang et al., 2016). In line, we observed that CD31+ cells derived from freshly dissociated human glioblastoma express αSMA *ex vivo.* In these cells, EDA+FN and EDB+FN gene silencing strongly reduced αSMA expression, suggesting a role for oncofetal FN

in promoting the expression of αSMA favoring the EndMT process in glioblastoma-derived endothelial cells (Fig. 1F). Similarly, a role for EDA+FN in promoting the conversion of fibroblastic precursors into myofibroblasts expressing αSMA has been reported (Muro et al., 2008; Serini et al., 1998; White et al., 2008).

Glioblastomas are characterized by high vascular density and vascular abnormalization with the typical formation of glomeruloid vascular structures (Wen and Kesari, 2008). All TGF-β isoforms and most abundantly TGF-β1 and TGF-β2 are expressed in glioblastoma (Frei et al., 2015), and they have been attributed a central role in both tumor angiogenesis and vessel remodeling. A direct role for TGF-β2 in regulating the phenotype of glioblastoma vessels, including the expression of components of the extracellular matrix, has been proposed. Indeed SMAD2/SMAD4 and SMAD3/SMAD4 complexes localize mainly to the vascular and perivascular areas in glioblastoma (Dieterich et al., 2012). TGF-β induces FN in several cell types (Ignotz and Massague, 1986) and is one of the best characterized modulators of the alternative splicing affecting the EDA and EDB domains (Balza et al., 1988; Borsi et al., 1990; Viedt et al., 1995). Here we show a trend of positive correlation in the expression of the three TGF-β isoforms and EDA+FN and EDB+FN in CD31+ cells derived from freshly dissociated human glioblastoma (Fig. 2). Also, we observed positive correlations in the expression of all TGF-β isoforms and FN, EDA+FN and EDB+FN in the αSMA+ cells fraction (Fig. 2). Notably, our studies reveal that TGF-β1, TGF-β2 and TGF-β3 induce FN, EDA+FN, and EDB+FN in hCMEC cells (Fig. 3). Here, induction of FN, EDA+FN, and EDB+FN by TGF-β involves the SMAD-dependent/canonical TGF-β signaling pathway and specifically SMAD3 (Fig. 3). *In vitro* experiments performed in CD31+ cells derived from freshly dissociated human glioblastoma revealed inter-patient variability, since TGF-β induced FN, EDA+FN and EDB+FN only in two out of the three cell line models derived from these patients (Fig. 4). We did not observe an inducibility of FN and oncofetal FN by TGF-β in the third primary cell line tested (ZH-616), but endogenous expression levels of oncofetal FN were dependent on SMAD3 and SMAD4. Thus, our data support a role for TGF-β/SMAD3/SMAD4-signaling in (oncofetal) FN expression in endothelial cells (Figs 3, 4).

In both CD31+ and αSMA+ cells, we also observed a positive correlation in the expression of TGFBI and FN, EDA+FN and EDB+FN (Fig. 2). TGFBI is an extracellular matrix glycoprotein, interacting with FN (Billings et al., 2002), induced by

TGF-β and previously reported to be up-regulated in glioblastoma vasculature (Mustafa et al., 2012). Strong positive correlations in the expression of TGFBI and FN have been reported in other contexts such as ovarian cancer (Ahmed et al., 2007). In addition, we observed positive correlations in the expression of FN and LTBP molecules (Fig. 2), the last ones being ECM molecules that bind to FN and that play a central role in the control of TGF-β latency and activation (Robertson et al., 2015). Overall, the positive correlations in the expression of the ECM-localized TGF-β target genes FN and TGFBI, as well as in the expression of ECM components involved in TGF-β storage and activation i.e. FN and LTBP, suggest a coordinated expression in the major ECM glycoproteins associated with TGF-β activity (Gopal et al., 2017) in glioblastoma vasculature.

The potential role played by oncofetal FN in neo-angiogenesis and vascular morphogenesis is still unclear. Double null mice for EDA and EDB domains die at embryonic stage with several vascular defects (Astrof et al., 2007). By contrast, single knockout mice for EDA and EDB containing FN isoforms are vital, show normal vasculogenesis (Fukuda et al., 2002; Muro et al., 2008) and normal physiological and tumor angiogenesis (Astrof et al., 2004). Since EDA/EDB null mice have phenotypical similarities with knockout mice for different growth factors including TGF-β1 (Kulkarni et al., 1995), a role for the EDA and EDB domains of FN in regulating TGF-β signaling has been postulated (Astrof and Hynes, 2009). In the present work, we demonstrate that gene silencing of EDA+FN and EDB+FN in hCMEC reduces the levels of phosphorylated SMAD1,5, in addition pSMAD3 levels were reduced upon EDA+FN-gene silencing as well (Fig. 5A). Interestingly, gene-silencing of EDB+FN in hCMEC and to a larger extent gene silencing of EDA+FN reduced levels of TGF-β1 in the conditioned media of these cells (Fig. 5B). This explains the reduction in pSMAD3 levels and suggests a role for FN and its splice variants in the control of TGF-β signaling in the ECM by affecting TGF-β latency/activation. Also, treatment of hCMEC with recombinant fragments of FN including the EDA and EDB domains reduced SMAD1,5 phosphorylation on both basal levels and upon TGF-β2 treatment when compared to untreated cells or cells treated with the FN fragments lacking the EDA and EDB domains (Fig. 5D,E). The same FN fragments also attenuated the induction of pSMAD2,3 upon TGF-β2 treatment. Overall these data suggest that the EDA and EDB domains of FN modulate the TGF-β superfamily signaling in hCMEC. Similarly, in fibroblasts a role

for EDA+FN in controlling TGF-β activation has been reported (Muro et al., 2008; Serini et al., 1998; White et al., 2008).

In summary, we show that EDA+FN and EDB+FN are abundantly expressed in glioblastoma vasculature and that both endothelial cells and pericytes/SVMC contribute to the expression of oncofetal FN in glioblastoma. In both CD31+ and αSMA+ cells TGF-β expression correlates with EDA+FN and EDB+FN expression. All TGF-β isoforms induce FN, EDA+FN, and EDB+FN in hCMEC and CD31+ cells derived from human glioblastoma tissues involving SMAD3/SMAD4. In turn, EDA+FN and EDB+FN modulate TGF-β superfamily signaling mainly affecting the SMAD1,5 signaling branch which also depends on other TGF-β superfamily members than the isoforms TGF-β1, TGF-β2 and TGF-β3. Since TGF-β superfamily ligands play a central role in vasculogenesis and angiogenesis, further studies are needed to deepen our knowledge on this new mode of regulation of TGF-β superfamily signaling in neo-vessels involving oncofetal FN.

MATERIAL AND METHODS

Real-time PCR (RT-PCR)

RT-PCR was performed using the primers reported in table S1. mRNA levels were determined by using the ΔC_T method and ARF1 as housekeeping gene.

Single-cell quantitative real-time polymerase chain reaction (qRT-PCR)

Glioblastoma tissues obtained from surgery were immediately dissociated using a papain-based dissociation system (Worthington, Lakewood, NJ, USA). Leukocytes were depleted using anti-human CD45 microbeads (Milteny Biotech, Bergisch Gladbach, Germany). Single-cell qRT-PCR gene expression profiling was performed using the C1 Single-Cell Autoprep and BioMark HD instruments (Fluidigm, South San Francisco, CA, USA). Cells were captured on a C1 Single-Cell Preamp IFC (10–17 µm) using the Fluidigm C1 and capture efficiency was evaluated under an inverted microscope to identify empty sites, sites with debris and multiple cells to exclude them from the final analysis. Preamplified cDNA was generated using the Single Cells-to-CT Kit (Life Technologies, Carlsbad, CA, USA), pooled qPCR primers (Table S1) and Fluidigm STA reagents. Preamplified cDNA was then used for high-

throughput qPCR measurement of each amplicon using the BioMark HD system with IFC Controller HX (Fluidigm) and 2X SsoFast EvaGreen Supermix with Low ROX (Bio-Rad, Hercules, CA, USA). Single-cell expression data were collected using the Fluidigm Data Collection software. Quality controls included cDNAs derived from a whole glioblastoma tumor before and after CD45+ depletion and the qPCR Human Reference cDNA, random-primed (Clontech, Mountain View, CA, USA). For all tumors tested runs were performed successfully. All primers used were tested for amplification efficiency of at least 90% by generating standard curves for each gene. Data was processed via removal of cells with low overall expression values, identification of limits of detection for each analyzed gene and cell-to-cell median normalization as described previously (Livak et al., 2013). Informed consent was obtained from all patients and the analysis was performed according to the guidelines of the local ethics committees (Kantonale Ethikkommission Zürich, Switzerland, KEK-ZH-Nr./BASCE-Nr. 2016-00456).

Enzyme-linked immunosorbent assay

For the detection of soluble FN, EDA+FN and EDB+FN, BRAND Immunograde 96 well plates (Sigma-Aldrich, St. Louis, MO, USA) were coated with 20 µg/ml gelatin in PBS overnight at room temperature, washed with PBS, blocked with 2% bovine serum albumin (BSA) in PBS and then incubated with the conditioned culture media of cells cultured for 72. The conditioned media were tested at different dilutions in 2% BSA in order to make sure that the resulting readings were in the linear range. FN, EDA+FN, and EDB+FN were detected by using the IST-5 (Klein et al., 2003), IST-9 (Borsi et al., 1987) and C6 (Balza et al., 2009) antibodies, respectively, at the final concentration of 2 µg/ml in 2% BSA in PBS. For the detection of insoluble FN, EDA+FN and EDB+FN cells cultured for 72 h in 96 well plate were fixed with methanol, blocked with 2% BSA in PBS and incubated with 0.5 µg/ml IST5 or 2 µg/ml IST9 or C6. The HRP goat anti-mouse IgG (minimal cross-reactivity) antibody (405306, lot #B167518, BioLegend, San Diego, CA, USA) was used as secondary antibody. 3,3', 5,5' tetramethylbenzidine (TMB) (BD Bioscience, San Jose, CA, USA) was used as a reaction substrate. Data for soluble FN, EDA+FN and EDB+FN are expressed as the values of absorbance at 450 nm divided by the protein concentration as determined in the undiluted cell conditioned media by Bradford Assay (Bio-Rad). In case of insoluble FN, cells seeded in a second 96 well plate and

subjected to the same treatments for 72 h, were incubated for 3 h with 3-(4,5-dimethylthiazol-2-yl)-2,5-diphenyl tetrazolium bromide (MTT). After cell lysis the absorbance at 540 nm was measured and used to normalize the ELISA data.

Immunohistochemistry

For immunohistochemical analysis of FN and CD31, methanol-fixed 5 µm cryostat sections of ten human glioblastoma and of four human normal brain tissues derived from patients with epilepsy were used. The analysis was performed according to the guidelines of the local ethics committees (Kantonale Ethikkommission Zürich, Switzerland, KEK-ZH-Nr./BASCE-Nr. 2016-00456). For the staining of fibronectins sections were treated with the primary antibodies IST-5, IST-9 and C6 at the final concentration of 2 µg/ml, the peroxidase mouse IgG Vectastain ABC kit (PK-4002, Vector Laboratories, Burlingame, CA, USA) and the DAB substrate (Peroxidase blocking, Dako-Agilent, Santa Clara, CA, USA). CD31+ positive cells were stained using the anti CD31+ monoclonal antibody clone JC70A (M0823, Lot#00063340, Dako, Glostrup, Denmark) diluted 1:40, the peroxidase mouse IgG Vectastain ABC kit (Vector Laboratories) and the DAB substrate (Dako-Agilent). For the αSMA IHC analysis, 5 µm formalin-fixed paraffin-embedded sections derived from two out of the six glioblastoma tissues employed also for the single-cell RT-PCR were used. Heat-induced epitope retrieval was performed in 10 mM Tris buffer, 1 mM EDTA, pH 9.0. Tissue sections were then treated with the anti αSMA monoclonal antibody clone 1A4 (A5228, batch 056M4828V, Sigma) diluted 1:50, the Histofine simple stain MAX PO (M) universal immuno-peroxidase polymer anti-mouse (414132F, Nichirei Biosciences, Tokyo, Japan) and the DAB substrate (Dako-Agilent). Serial section were stained for CD31 as above described after heat-induced epitope retrieval in 0.1 M citrate buffer pH 6.0. Images were acquired using an Axio Scope.A1 microscope equipped with an AxioCam MRc camera and the AxioVision LE64 program (Carl Zeiss, Oberkochen, Germany).

Immunoblot

Denatured and reduced (with 5% β-mercaptoethanol) whole cell lysates or denatured concentrated conditioned media under reducing or non-reducing conditions were separated by polyacrylamide gels and transferred to nitrocellulose membranes (Amersham/Ge Healthcare Life Science, Arlington Heights, IL, USA). Membranes

were blocked with 5% skimmed milk or serum bovine albumin (ApplChem, Darmstadt, Germany) and treated with the following primary antibodies: IST-4 (Sekiguchi et al., 1985), IST-9 and C6 (see above) antibodies to fibronectin used at the final concentration of 5 µg/ml; the antibodies specific for SMAD1 (9743, ref:01/2012), phosphorylated SMAD1/5 (pSmad1/5(Ser463/465)) (9516, ref.08/2015), SMAD2 (3122, ref:05/2015), phosphorylated SMAD2 (pSMAD2 (Ser465/467)) (3108, ref: 04/2016), SMAD3 (9513, ref: 07/2014), and SMAD4 (9515, ref:08/2013) from Cell Signaling Technology (Danvers, MA, USA), used diluted 1:1000 except for anti-pSMAD2 which was diluted 1:500; anti-phosphorylated SMAD3 (ab52903, lot#GR128879-24, Abcam, Cambridge, UK) diluted 1:1000; anti-human LAP/TGF-β1 (AF-246-NA, lot#EF0212101, R&D Systems, Minneapolis, MN, USA) diluted 1:2000, anti-TGF-β1 (G122A, lot#0000051912, Promega, Madison, WI, USA) diluted 1:1000, anti-GAPDH (EB07069, lot#C2, Everest Biotech, Ramona, CA, USA) at the final concentration of 0.2 µg/ml. Secondary antibodies used were HRP-coupled goat anti-rabbit (sc-2004, lot #B2216) or donkey anti-goat (sc-2033, lot #A2914) (Santa Cruz Biotechnology, Dallas, TX, USA) or sheep anti-mouse antibodies (NA931V, lot #9997907, Ge Healthcare UK Limited, Amersham, UK), diluted 1:5000. Protein bands were visualized with horseradish peroxidase (HRP)-coupled secondary antibodies followed by enhanced chemiluminescence (Pierce/Thermo Fisher, Madison, WI, USA).

Cell culture

Human cerebral microvascular endothelial cells (hCMEC-D3) were kindly provided by P.C. Couraud (Paris, France). The human glioblastoma-derived CD31+ cell line ZH-459, ZH-464, and ZH-483-2 have been reported (Krishnan et al., 2015). The human glioblastoma-derived CD31+ cell lines ZH-613 and ZH-616 were prepared as described (Krishnan et al., 2015). Endothelial cells were cultured in EBM-2 medium (CC-3156, Lonza, Walkersville, MD), containing 0.1 M HEPES (Gibco), 1% v/v CD lipid concentrate (Gibco) and endothelial growth supplements (EGM-2-CC4176, Lonza). HCMEC-D3 were negatively tested for contamination with mycoplasma. Glioblastoma-derived cell lines were not tested for contamination and were not recently authenticated because they were used at low passage number. Informed consent was obtained from all patients.

Reagents

Transient gene silencing was performed by using the Lipofectamine RNAiMAX reagent (Invitrogen/Life Technologies) and the following siRNA provided by Dharmacon (Lafayette, CO, USA): ON-TARGETplus, siRNA SMART pools specific for SMAD2 (L-003561-00), SMAD3 (L-020067-00), SMAD4 (L-003902-00), TGF-βRII (L-003930–00), ALK1 (L-005302–02), ALK5 (L-003929–00), TGF-β1 (L-012562-00) and non-targeting control (D-001810-10) at a final concentration of 100 nM. For EDA+FN and EDB+FN the following siRNA provided by Dharmacon and used at the final concentration of 10nM were used: 1) EDA+FN: pool of siEDA1 5'-GGTTCTGAGTACACAGTCA-3' and siEDA2 5'- GGTTCTGAGTACACAGTCA 3'; 2) EDB+FN: a pool of four siRNA previously described (Khan et al., 2005).

Cells were treated using the following reagents in EBM-2 medium without supplements: 5 ng/ml TGF-β1, TGF-β2 or TGF-β3 (R&D Systems, Minneapolis, MN, USA), 1 μM SD-208 (Scios, Fremont, CA, USA) and 10 μM SP600125 (Sigma-Aldrich). The human fibronectin recombinant fragments used in this study were previously described (Carnemolla et al., 1996).

Statistical analysis

All experiments were performed at least twice and in triplicates. Statistical analysis for the scRT-PCR data was performed in R using the package *ggplot2*. All other statistical analysis was performed by using the GraphPad Prism 5 program. Data are shown as the mean ± the standard deviation (SD). The statistical significance of the RT-PCR and ELISA data was determined by performing one-way ANOVA followed by Tukey's post hoc test at 95% confidence interval (CI).

ABBREVIATIONS

Transforming growth factor (TGF)-β; fibronectin (FN); extra-domain A (EDA); extra-domain B (EDB); extracellular matrix (ECM); activin-like kinase (ALK); bone morphogenetic proteins (BMP); alpha-smooth muscle actin (αSMA); vascular smooth muscle cells (VSMC); transforming growth factor-β induced (TGFBI); latent TGF-β binding protein (LTBP); latency-associated peptide (LAP); small latent complex (SLC); large latent complex (LLC) ; human cerebral microvascular endothelial cells (hCMEC); single-cell real-time polymerase chain reaction (scRT-PCR).

ACKNOWLEDGMENTS

We thank Prof. Elisabeth Jane Rushing from the Institute of Neuropathology of the University Hospital of Zurich for providing glioblastoma tissues.

COMPETING INTERESTS

MW has received research grants from Acceleron, Actelion, Alpinia Institute, Bayer, Isarna, Merk, Sharp & Dohme (MSD), Merck (EMD), Novocure, Piqur Therapeutics, and Roche and honoraria for lectures or advisory board participation or consulting from Celldex, Immunocellular Therapeutics, MSD, Merck (EMD), Novocure, Pfizer, Roche, and Teva. LZ is CEO of Sirius-biotech a biotechnology start-up; CC is a scientist of Sirius-biotech. The other authors have no financial conflicts of interest.

AUTHOR CONTRIBUTIONS

Conceived and designed the experiments: EV, MW, IB. Performed the experiments: EV, KE, CC. Analyzed the scRT-PCR data: WM, MC. Analyzed the other data: EV, MW, CB, LZ, IB. Wrote the manuscript: EV, MW, IB. Reviewed the manuscript: EV, MW, LZ, IB.

FUNDING

This work was supported by the program Highly Specialized Medicine (HSM) 2 of the Canton of Zurich, Switzerland to MW, by the Swiss Cancer League/Oncosuisse [project number KFS-3305-08-2013 to IB and MW], by the "EMDO STIFTUNG Zürich" [Project number 808 to IB] and by a donor of the foundation of the University of Zurich (UZH Foundation). CB's research is funded by SystemsX.ch, the Swiss initiative for systems biology

REFERENCES

Ahmed, A. A., Mills, A. D., Ibrahim, A. E., Temple, J., Blenkiron, C., Vias, M., Massie, C. E., Iyer, N. G., McGeoch, A., Crawford, R. et al. (2007). The extracellular matrix protein TGFBI induces microtubule stabilization and sensitizes ovarian cancers to paclitaxel. *Cancer Cell* **12**, 514-27.

Astrof, S., Crowley, D., George, E. L., Fukuda, T., Sekiguchi, K., Hanahan, D. and Hynes, R. O. (2004). Direct test of potential roles of EIIIA and EIIIB alternatively spliced segments of fibronectin in physiological and tumor angiogenesis. *Mol Cell Biol* **24**, 8662-70.

Astrof, S., Crowley, D. and Hynes, R. O. (2007). Multiple cardiovascular defects caused by the absence of alternatively spliced segments of fibronectin. *Dev Biol* **311**, 11-24.

Astrof, S. and Hynes, R. O. (2009). Fibronectins in vascular morphogenesis. *Angiogenesis* **12**, 165-75.

Balza, E., Borsi, L., Allemanni, G. and Zardi, L. (1988). Transforming growth factor beta regulates the levels of different fibronectin isoforms in normal human cultured fibroblasts. *FEBS Lett* **228**, 42-4.

Balza, E., Sassi, F., Ventura, E., Parodi, A., Fossati, S., Blalock, W., Carnemolla, B., Castellani, P., Zardi, L. and Borsi, L. (2009). A novel human fibronectin cryptic sequence unmasked by the insertion of the angiogenesis-associated extra type III domain B. *Int J Cancer* **125**, 751-8.

Billings, P. C., Whitbeck, J. C., Adams, C. S., Abrams, W. R., Cohen, A. J., Engelsberg, B. N., Howard, P. S. and Rosenbloom, J. (2002). The transforming growth factor-beta-inducible matrix protein (beta)ig-h3 interacts with fibronectin. *J Biol Chem* **277**, 28003-9.

Borsi, L., Balza, E., Bestagno, M., Castellani, P., Carnemolla, B., Biro, A., Leprini, A., Sepulveda, J., Burrone, O., Neri, D. et al. (2002). Selective targeting of tumoral vasculature: comparison of different formats of an antibody (L19) to the ED-B domain of fibronectin. *Int J Cancer* **102**, 75-85.

Borsi, L., Balza, E., Carnemolla, B., Sassi, F., Castellani, P., Berndt, A., Kosmehl, H., Biro, A., Siri, A., Orecchia, P. et al. (2003). Selective targeted delivery of TNFalpha to tumor blood vessels. *Blood* **102**, 4384-92.

Borsi, L., Carnemolla, B., Castellani, P., Rosellini, C., Vecchio, D., Allemanni, G., Chang, S. E., Taylor-Papadimitriou, J., Pande, H. and Zardi, L.

(1987). Monoclonal antibodies in the analysis of fibronectin isoforms generated by alternative splicing of mRNA precursors in normal and transformed human cells. *J Cell Biol* **104**, 595-600.

Borsi, L., Castellani, P., Risso, A. M., Leprini, A. and Zardi, L. (1990). Transforming growth factor-beta regulates the splicing pattern of fibronectin messenger RNA precursor. *FEBS Lett* **261**, 175-8.

Carnemolla, B., Balza, E., Siri, A., Zardi, L., Nicotra, M. R., Bigotti, A. and Natali, P. G. (1989). A tumor-associated fibronectin isoform generated by alternative splicing of messenger RNA precursors. *J Cell Biol* **108**, 1139-48.

Carnemolla, B., Borsi, L., Balza, E., Castellani, P., Meazza, R., Berndt, A., Ferrini, S., Kosmehl, H., Neri, D. and Zardi, L. (2002). Enhancement of the antitumor properties of interleukin-2 by its targeted delivery to the tumor blood vessel extracellular matrix. *Blood* **99**, 1659-65.

Carnemolla, B., Neri, D., Castellani, P., Leprini, A., Neri, G., Pini, A., Winter, G. and Zardi, L. (1996). Phage antibodies with pan-species recognition of the oncofoetal angiogenesis marker fibronectin ED-B domain. *Int J Cancer* **68**, 397-405.

Castellani, P., Borsi, L., Carnemolla, B., Biro, A., Dorcaratto, A., Viale, G. L., Neri, D. and Zardi, L. (2002). Differentiation between high- and low-grade astrocytoma using a human recombinant antibody to the extra domain-B of fibronectin. *Am J Pathol* **161**, 1695-700.

Castellani, P., Viale, G., Dorcaratto, A., Nicolo, G., Kaczmarek, J., Querze, G. and Zardi, L. (1994). The fibronectin isoform containing the ED-B oncofetal domain: a marker of angiogenesis. *Int J Cancer* **59**, 612-8.

Clavreul, A., Etcheverry, A., Chassevent, A., Quillien, V., Avril, T., Jourdan, M. L., Michalak, S., Francois, P., Carre, J. L., Mosser, J. et al. (2012). Isolation of a new cell population in the glioblastoma microenvironment. *J Neurooncol* **106**, 493-504.

Constam, D. B. (2014). Regulation of TGFbeta and related signals by precursor processing. *Semin Cell Dev Biol* **32**, 85-97.

Danielli, R., Patuzzo, R., Di Giacomo, A. M., Gallino, G., Maurichi, A., Di Florio, A., Cutaia, O., Lazzeri, A., Fazio, C., Miracco, C. et al. (2015). Intralesional administration of L19-IL2/L19-TNF in stage III or stage IVM1a melanoma patients: results of a phase II study. *Cancer Immunol Immunother* **64**, 999-1009.

Dieterich, L. C., Mellberg, S., Langenkamp, E., Zhang, L., Zieba, A., Salomaki, H., Teichert, M., Huang, H., Edqvist, P. H., Kraus, T. et al. (2012). Transcriptional profiling of human glioblastoma vessels indicates a key role of VEGF-A and TGFbeta2 in vascular abnormalization. *J Pathol* **228**, 378-90.

Erba, P. A., Sollini, M., Orciuolo, E., Traino, C., Petrini, M., Paganelli, G., Bombardieri, E., Grana, C., Giovannoni, L., Neri, D. et al. (2012). Radioimmunotherapy with radretumab in patients with relapsed hematologic malignancies. *J Nucl Med* **53**, 922-7.

Ffrench-Constant, C., Van de Water, L., Dvorak, H. F. and Hynes, R. O. (1989). Reappearance of an embryonic pattern of fibronectin splicing during wound healing in the adult rat. *J Cell Biol* **109**, 903-14.

Frei, K., Gramatzki, D., Tritschler, I., Schroeder, J. J., Espinoza, L., Rushing, E. J. and Weller, M. (2015). Transforming growth factor-beta pathway activity in glioblastoma. *Oncotarget* **6**, 5963-77.

Fukuda, T., Yoshida, N., Kataoka, Y., Manabe, R., Mizuno-Horikawa, Y., Sato, M., Kuriyama, K., Yasui, N. and Sekiguchi, K. (2002). Mice lacking the EDB segment of fibronectin develop normally but exhibit reduced cell growth and fibronectin matrix assembly in vitro. *Cancer Res* **62**, 5603-10.

Gopal, S., Veracini, L., Grall, D., Butori, C., Schaub, S., Audebert, S., Camoin, L., Baudelet, E., Radwanska, A., Beghelli-de la Forest Divonne, S. et al. (2017). Fibronectin-guided migration of carcinoma collectives. *Nat Commun* **8**, 14105.

Goumans, M. J., Valdimarsdottir, G., Itoh, S., Rosendahl, A., Sideras, P. and ten Dijke, P. (2002). Balancing the activation state of the endothelium via two distinct TGF-beta type I receptors. *EMBO J* **21**, 1743-53.

Hocevar, B. A., Brown, T. L. and Howe, P. H. (1999). TGF-beta induces fibronectin synthesis through a c-Jun N-terminal kinase-dependent, Smad4-independent pathway. *EMBO J* **18**, 1345-56.

Huang, M., Liu, T., Ma, P., Mitteer, R. A., Jr., Zhang, Z., Kim, H. J., Yeo, E., Zhang, D., Cai, P., Li, C. et al. (2016). c-Met-mediated endothelial plasticity drives aberrant vascularization and chemoresistance in glioblastoma. *J Clin Invest* **126**, 1801-14.

Hynes, R. O. (1990). Fibronectins: New York: Springer-Verlag.

Ignotz, R. A. and Massague, J. (1986). Transforming growth factor-beta stimulates the expression of fibronectin and collagen and their incorporation into the extracellular matrix. *J Biol Chem* **261**, 4337-45.

Khan, Z. A., Chan, B. M., Uniyal, S., Barbin, Y. P., Farhangkhoee, H., Chen, S. and Chakrabarti, S. (2005). EDB fibronectin and angiogenesis -- a novel mechanistic pathway. *Angiogenesis* **8**, 183-96.

Klein, R. M., Zheng, M., Ambesi, A., Van De Water, L. and McKeown-Longo, P. J. (2003). Stimulation of extracellular matrix remodeling by the first type III repeat in fibronectin. *J Cell Sci* **116**, 4663-74.

Krishnan, S., Szabo, E., Burghardt, I., Frei, K., Tabatabai, G. and Weller, M. (2015). Modulation of cerebral endothelial cell function by TGF-beta in glioblastoma: VEGF-dependent angiogenesis versus endothelial mesenchymal transition. *Oncotarget* **6**, 22480-95.

Kulkarni, A. B., Ward, J. M., Yaswen, L., Mackall, C. L., Bauer, S. R., Huh, C. G., Gress, R. E. and Karlsson, S. (1995). Transforming growth factor-beta 1 null mice. An animal model for inflammatory disorders. *Am J Pathol* **146**, 264-75.

Liu, I. M., Schilling, S. H., Knouse, K. A., Choy, L., Derynck, R. and Wang, X. F. (2009). TGFbeta-stimulated Smad1/5 phosphorylation requires the ALK5 L45 loop and mediates the pro-migratory TGFbeta switch. *EMBO J* **28**, 88-98.

Livak, K. J., Wills, Q. F., Tipping, A. J., Datta, K., Mittal, R., Goldson, A. J., Sexton, D. W. and Holmes, C. C. (2013). Methods for qPCR gene expression profiling applied to 1440 lymphoblastoid single cells. *Methods* **59**, 71-9.

Massague, J. (2012). TGFbeta signalling in context. *Nat Rev Mol Cell Biol* **13**, 616-30.

Moustakas, A. and Heldin, C. H. (2005). Non-Smad TGF-beta signals. *J Cell Sci* **118**, 3573-84.

Muro, A. F., Moretti, F. A., Moore, B. B., Yan, M., Atrasz, R. G., Wilke, C. A., Flaherty, K. R., Martinez, F. J., Tsui, J. L., Sheppard, D. et al. (2008). An essential role for fibronectin extra type III domain A in pulmonary fibrosis. *Am J Respir Crit Care Med* **177**, 638-45.

Mustafa, D. A., Dekker, L. J., Stingl, C., Kremer, A., Stoop, M., Sillevis Smitt, P. A., Kros, J. M. and Luider, T. M. (2012). A proteome comparison between physiological angiogenesis and angiogenesis in glioblastoma. *Mol Cell Proteomics* **11**, M111 008466.

Neri, D. and Bicknell, R. (2005). Tumour vascular targeting. *Nat Rev Cancer* **5**, 436-46.

Pankov, R. and Yamada, K. M. (2002). Fibronectin at a glance. *J Cell Sci* **115**, 3861-3.

Pardali, E. and ten Dijke, P. (2009). Transforming growth factor-beta signaling and tumor angiogenesis. *Front Biosci (Landmark Ed)* **14**, 4848-61.

Poli, G. L., Bianchi, C., Virotta, G., Bettini, A., Moretti, R., Trachsel, E., Elia, G., Giovannoni, L., Neri, D. and Bruno, A. (2013). Radretumab radioimmunotherapy in patients with brain metastasis: a 124I-L19SIP dosimetric PET study. *Cancer Immunol Res* **1**, 134-43.

Robertson, I. B., Horiguchi, M., Zilberberg, L., Dabovic, B., Hadjiolova, K. and Rifkin, D. B. (2015). Latent TGF-beta-binding proteins. *Matrix Biol* **47**, 44-53.

Rodon, L., Gonzalez-Junca, A., Inda Mdel, M., Sala-Hojman, A., Martinez-Saez, E. and Seoane, J. (2014). Active CREB1 promotes a malignant TGFbeta2 autocrine loop in glioblastoma. *Cancer Discov* **4**, 1230-41.

Rybak, J. N., Roesli, C., Kaspar, M., Villa, A. and Neri, D. (2007). The extra-domain A of fibronectin is a vascular marker of solid tumors and metastases. *Cancer Res* **67**, 10948-57.

Santimaria, M., Moscatelli, G., Viale, G. L., Giovannoni, L., Neri, G., Viti, F., Leprini, A., Borsi, L., Castellani, P., Zardi, L. et al. (2003). Immunoscintigraphic detection of the ED-B domain of fibronectin, a marker of angiogenesis, in patients with cancer. *Clin Cancer Res* **9**, 571-9.

Schwarzbauer, J. E. (1991). Alternative splicing of fibronectin: three variants, three functions. *Bioessays* **13**, 527-33.

Sekiguchi, K., Siri, A., Zardi, L. and Hakomori, S. (1985). Differences in domain structure between human fibronectins isolated from plasma and from culture supernatants of normal and transformed fibroblasts. Studies with domain-specific antibodies. *J Biol Chem* **260**, 5105-14.

Serini, G., Bochaton-Piallat, M. L., Ropraz, P., Geinoz, A., Borsi, L., Zardi, L. and Gabbiani, G. (1998). The fibronectin domain ED-A is crucial for myofibroblastic phenotype induction by transforming growth factor-beta1. *J Cell Biol* **142**, 873-81.

Takeuchi, H., Hashimoto, N., Kitai, R., Kubota, T. and Kikuta, K. (2010). Proliferation of vascular smooth muscle cells in glioblastoma multiforme. *J Neurosurg* **113**, 218-24.

Tian, H., Mythreye, K., Golzio, C., Katsanis, N. and Blobe, G. C. (2012). Endoglin mediates fibronectin/alpha5beta1 integrin and TGF-beta pathway crosstalk in endothelial cells. *EMBO J* **31**, 3885-900.

Uhl, M., Aulwurm, S., Wischhusen, J., Weiler, M., Ma, J. Y., Almirez, R., Mangadu, R., Liu, Y. W., Platten, M., Herrlinger, U. et al. (2004). SD-208, a novel transforming growth factor beta receptor I kinase inhibitor, inhibits growth and invasiveness and enhances immunogenicity of murine and human glioma cells in vitro and in vivo. *Cancer Res* **64**, 7954-61.

Viedt, C., Burger, A. and Hansch, G. M. (1995). Fibronectin synthesis in tubular epithelial cells: up-regulation of the EDA splice variant by transforming growth factor beta. *Kidney Int* **48**, 1810-7.

Wang, J., Cazzato, E., Ladewig, E., Frattini, V., Rosenbloom, D. I., Zairis, S., Abate, F., Liu, Z., Elliott, O., Shin, Y. J. et al. (2016). Clonal evolution of glioblastoma under therapy. *Nat Genet* **48**, 768-76.

Wen, P. Y. and Kesari, S. (2008). Malignant gliomas in adults. *N Engl J Med* **359**, 492-507.

White, E. S., Baralle, F. E. and Muro, A. F. (2008). New insights into form and function of fibronectin splice variants. *J Pathol* **216**, 1-14.

Zardi, L., Carnemolla, B., Siri, A., Petersen, T. E., Paolella, G., Sebastio, G. and Baralle, F. E. (1987). Transformed human cells produce a new fibronectin isoform by preferential alternative splicing of a previously unobserved exon. *Embo J* **6**, 2337-42.

Zardi, L., Cianfriglia, M., Balza, E., Carnemolla, B., Siri, A. and Croce, C. M. (1982). Species-specific monoclonal antibodies in the assignment of the gene for human fibronectin to chromosome 2. *EMBO J* **1**, 929-33.

Zegers, C. M., Rekers, N. H., Quaden, D. H., Lieuwes, N. G., Yaromina, A., Germeraad, W. T., Wieten, L., Biessen, E. A., Boon, L., Neri, D. et al. (2015). Radiotherapy combined with the immunocytokine L19-IL2 provides long-lasting antitumor effects. *Clin Cancer Res* **21**, 1151-60.

Zhang, L., Zhou, F. and ten Dijke, P. (2013). Signaling interplay between transforming growth factor-beta receptor and PI3K/AKT pathways in cancer. *Trends Biochem Sci* **38**, 612-20.

Figures

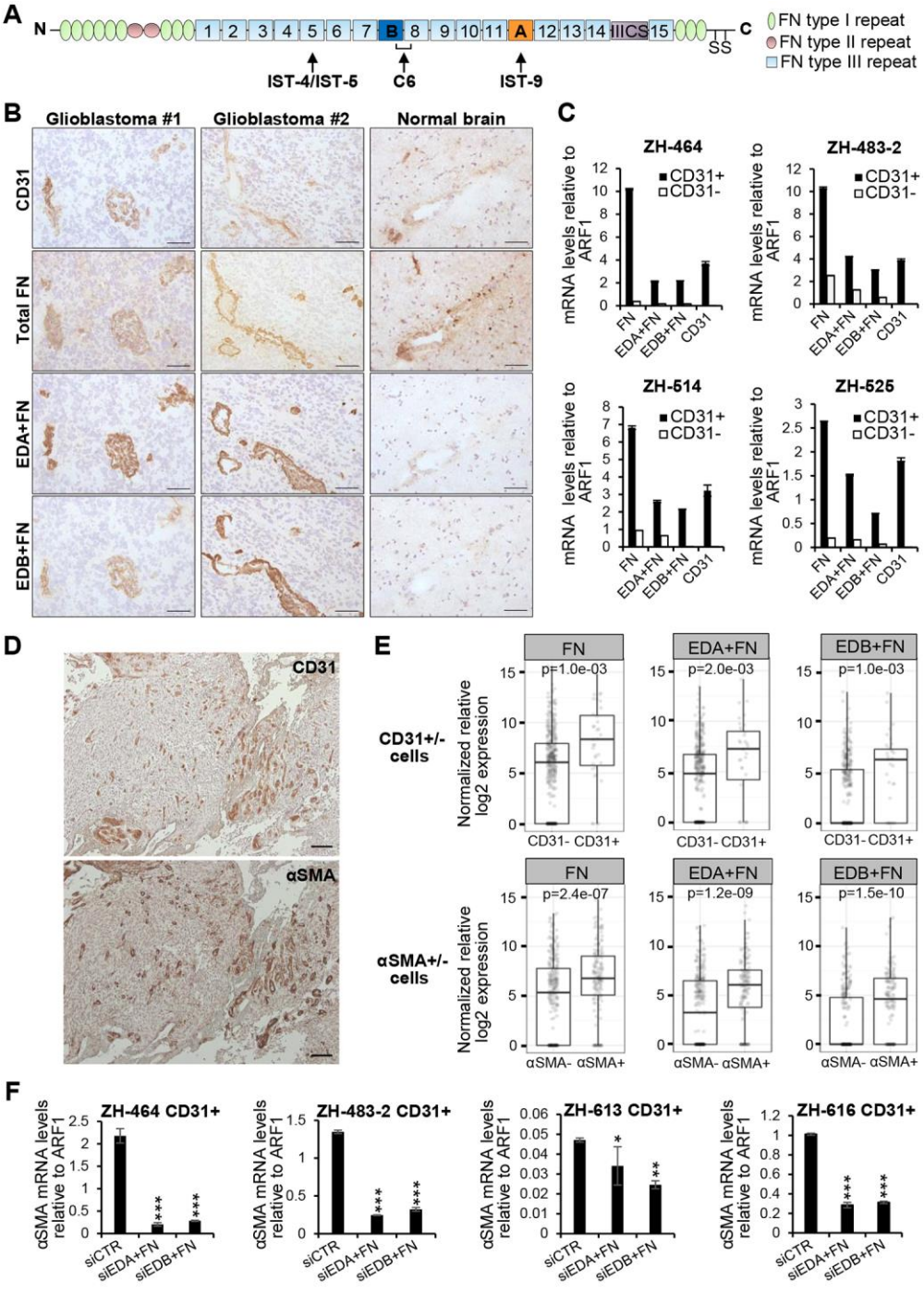

Figure 1. EDA+FN and EDB+FN are expressed in glioblastoma blood vessels. **A.** Schematic representation of the modular structure of FN. The target regions of the monoclonal antibodies specific for the FN type III repeat 5 (IST-4 and IST-5), EDA+FN (IST-9) and EDB+FN (C6) are indicated. **B.** CD31, total FN, EDA+FN and EDB+FN were detected immunohistochemically in frozen glioblastoma sections and in frozen normal brain sections obtained from epilepsy surgery. Representative

photomicrographs of two glioblastoma patients and one of the patients suffering from epilepsy are shown, bars indicate 50 µm. **C.** Total FN, EDA+FN and EDB+FN mRNA levels were determined in CD31+ *vs.* CD31- cells isolated from freshly dissociated glioblastoma tissues by RT-PCR. The "ZH" headings refer to codes for individual patients. Data are mean of technical triplicates ± SD. **D.** CD31 and αSMA were immunohistochemically detected in paraffin-embedded glioblastoma sections. Bars indicate 100 µm. **E.** Normalized relative gene expression on a log2 scale of FN, EDA+FN, and EDB+FN in individual cells derived from freshly dissociated human glioblastoma. Data from 6 individual tumors were pooled and cells were divided into CD31+ (N=35) and CD31- (N=430) (upper panels) and in αSMA+ (N=164) and αSMA- (N=301) (lower panels) subpopulations. Grey dots are all the actual data points. Boxes depict the median and interquartile ranges, whiskers extend to the largest value no further than 1.5-fold interquartile ranges from the hinge. In case of the CD31- and αSMA- cells the median values for EDB+FN are at 0. Two-sided t-test and Bonferroni adjustment for multiple testing were performed to compare gene expression in CD31+ *vs.* CD31- or αSMA+ *vs.* αSMA- cells. **F.** αSMA mRNA levels were determined by RT-PCR in the indicated CD31+ sub-cell lines upon specific gene silencing of EDA+FN, EDB+FN or non-targeting control. The "ZH" headings refer to codes for individual patients. Data are expressed as mean of technical triplicates ± SD (*p<.05, **p<.01, ***p<.001 one-way ANOVA followed by Tukey's post hoc test 95% CI).

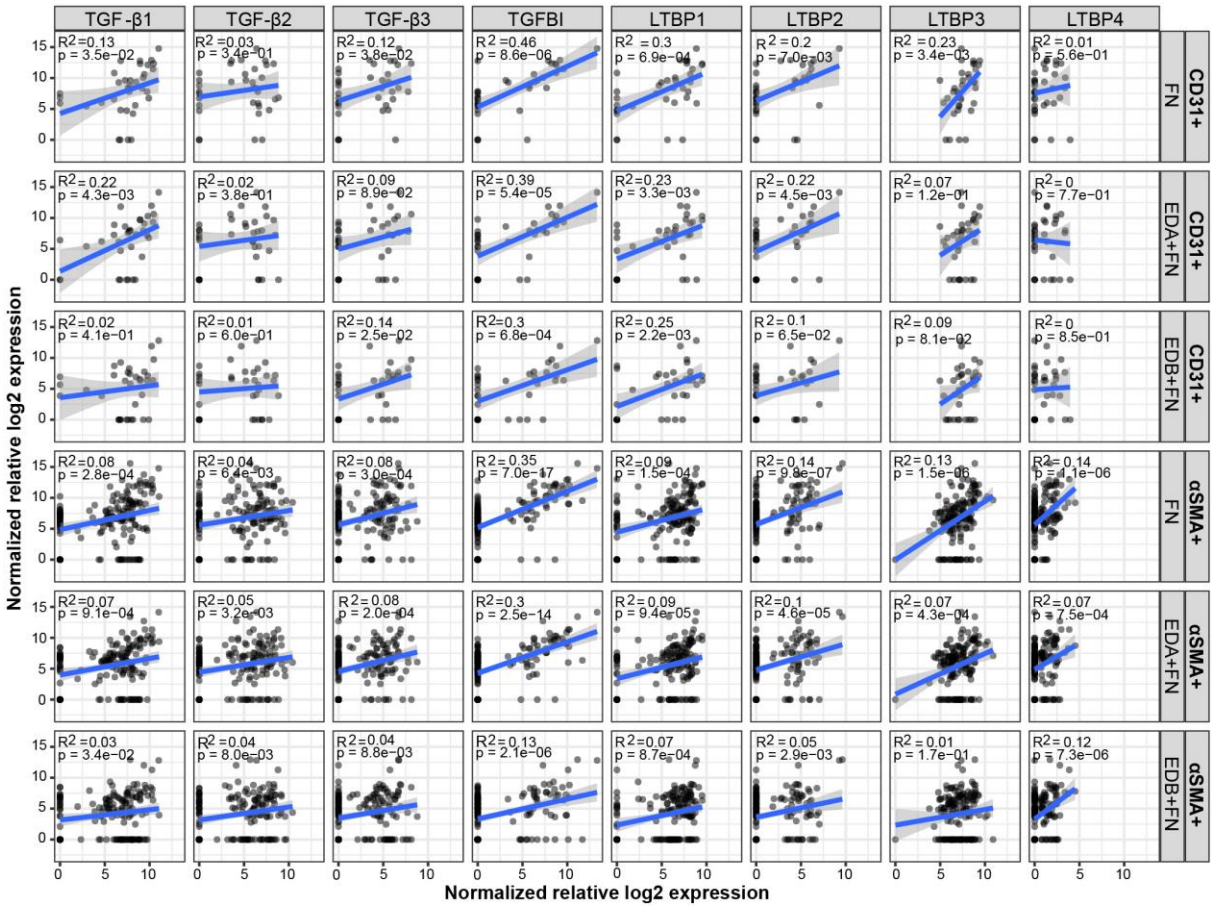

Figure 2. Positive correlations between the expression of TGF-β, TGF-β-induced (TGFBI), latent TGF-β binding proteins (LTBP) and of EDA+FN or EDB+FN on a single cell level in CD31+ and αSMA+ cells derived from human glioblastoma. Single cell RT-PCR in CD31+ (upper panels) and αSMA+ (lower panels) cells derived from freshly dissociated human glioblastoma (N=6). Data from the 6 individual patients were pooled. Dots are all the actual data points. X-axis: normalized relative log2 expression values of TGF-β1, TGF-β2, TGF-β3, TGFBI, LTBP1, LTBP2, LTBP3 and LTBP4; y-axis: normalized relative log2 expression values of FN, EDA+FN and EDB+FN. Correlations are indicated by slopes of blue lines. p-values are significance of the slope coefficient for each graph, Benjamini-Hochberg adjusted.

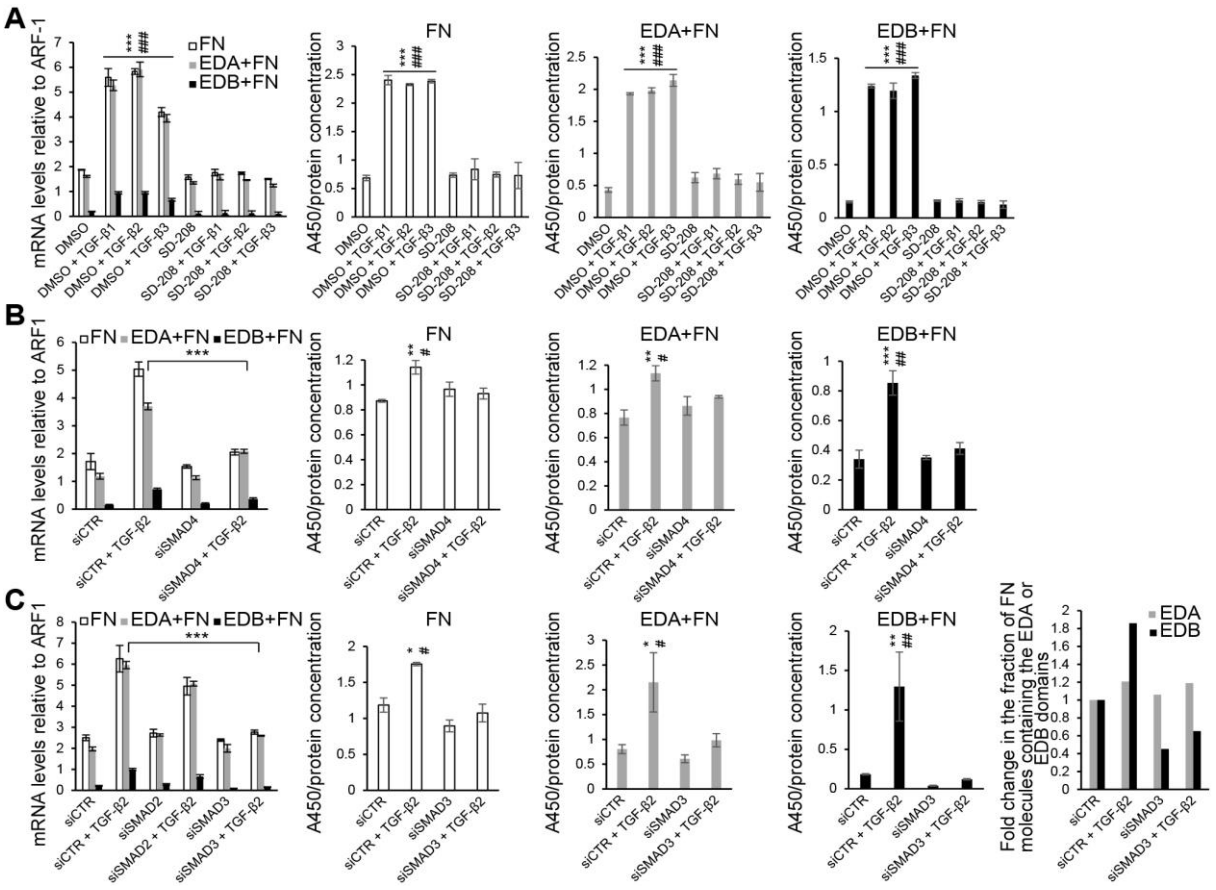

Figure 3. TGF-β1, TGF-β2 and TGF-β3 induce EDA+FN and EDB+FN expression in hCMEC in a TGF-βRI- and SMAD4/SMAD3-dependent manner. In all experiments FN, EDA+FN and EDB+FN levels were determined on mRNA level 48 h post TGF-β treatment by RT-PCR and on protein level in the conditioned media 72 h post TGF-β1, TGF-β2 or TGF-β3 treatment by ELISA. **A**. FN, EDA+FN and EDB+FN mRNA (left panel) and protein levels (other panels) in hCMEC cells incubated with 1 µM SD-208 or DMSO as solvent control for 1 h and then treated with 5 ng/ml TGF-β1, TGF-β2 or TGF-β3 (* DMSO + TGF-β1 or TGF-β2 or TGF-β3 *vs.* DMSO; # DMSO + TGFβ1 or TGFβ2 or TGF-β3 *vs.* SD-208 + TGF-β1 or TGF-β2 or TGF-β3). **B.** FN, EDA+FN and EDB+FN mRNA (left panel) and protein (other panels) levels in hCMEC transfected with siRNA targeting SMAD4 or non-targeting control and treated with 5 ng/ml TGF-β2 24 h post-transfection (ELISA data: * siCTR + TGF-β2 *vs.* siCTR; # siCTR + TGFβ2 *vs.* siSMAD4 + TGF-β2). **C.** FN, EDA+FN and EDB+FN mRNA levels (left panel) in hCMEC transfected with siRNA targeting SMAD2, SMAD3 or non-targeting control and treated with 5 ng/ml TGF-β2 24 h post-transfection. FN, EDA+FN and EDB+FN protein levels in hCMEC transfected with siRNA targeting SMAD3 or non-targeting control and treated with 5 ng/ml TGF-β2 24

h post-transfection (central panels). The fold change in the fraction of FN molecules containing the EDA domain or EDB domain, using the RT-PCR data reported on the left panel, is indicated (right panel) (ELISA data:* siCTR + TGFβ2 *vs*. siCTR; # siCTR + TGFβ2 *vs*. siSMAD3 + TGFβ2). All experiments were repeated at least twice. Data are mean of triplicates (technical for RT-PCR data and biological for ELISA data) ± SD ($^{*/\#}p<.05$, $^{**/\#\#}p<.01$, $^{***/\#\#\#}p<.001$ one-way ANOVA followed by Tukey's post hoc test 95% CI).

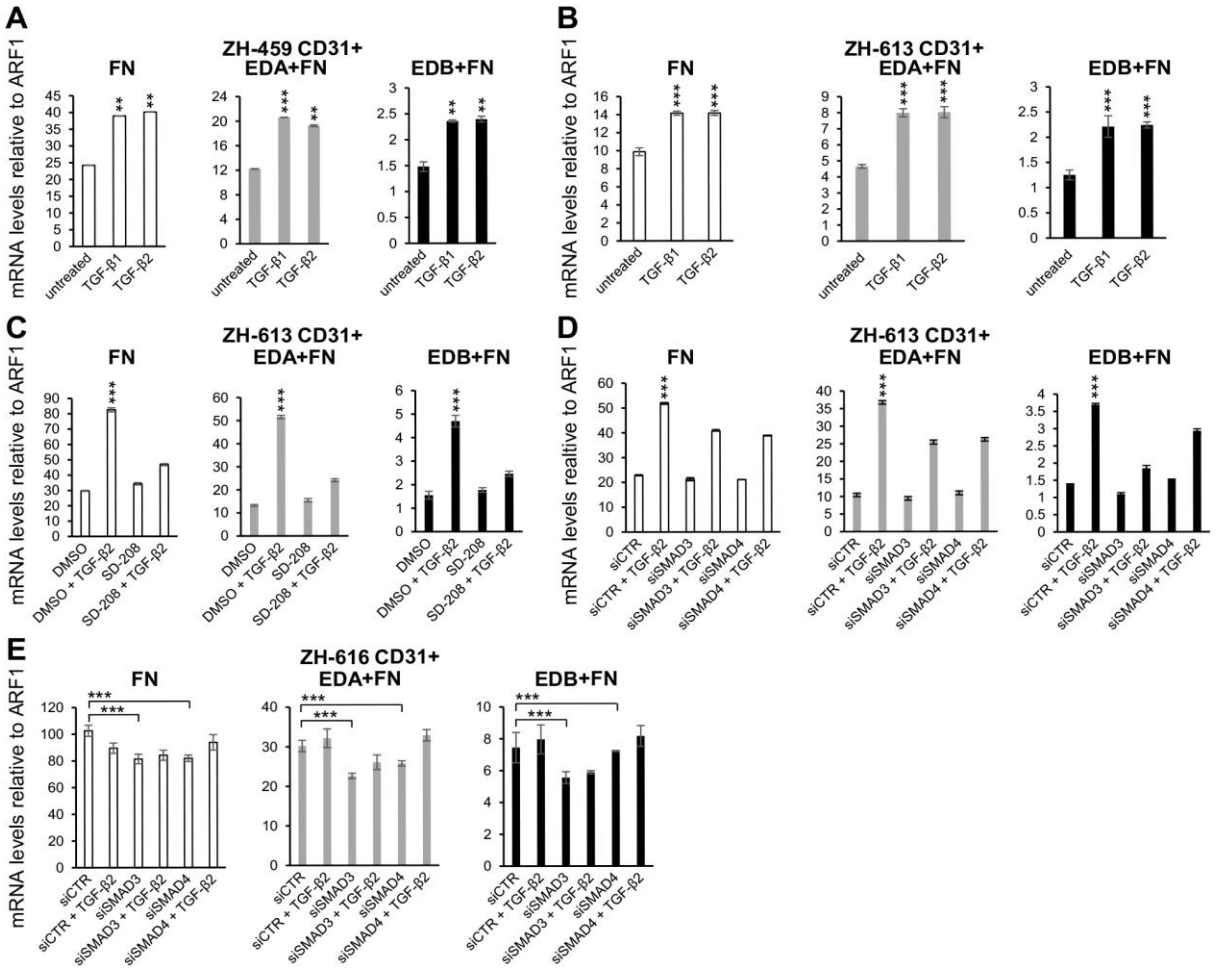

Figure 4. TGF-β1 and TGF-β2 induce EDA+FN and EDB+FN expression in CD31+ cells derived from glioblastoma in a TGF-βRI- and SMAD4/SMAD3-dependent manner. A-B. FN, EDA+FN and EDB+FN mRNA levels in ZH-459 CD31+ (A) and in ZH-613 CD31+ cells (B) treated with 5 ng/ml TGF-β1 or TGF-β2 for 48 h (* TGF-β1 or TGF-β2 *vs.* untreated). **C.** FN, EDA+FN and EDB+FN mRNA levels in ZH-613 CD31+ cells incubated for 1 h with 1 μM SD-208 or DMSO as solvent control and then treated with 5 ng/ml TGF-β2 for 48 h (* DMSO + TGF-β2 *vs.* all other samples). **D**-**E**. FN, EDA+FN and EDB+FN mRNA levels in ZH-613 CD31+ (D) and ZH-616 CD31+ (E) cells transfected with siRNA targeting SMAD3, SMAD4 or non-targeting control and then treated with 5 ng/ml TGF-β2 24 h post-transfection for 48 h (in D, * siCTR + TGF-β2 *vs.* all other samples). The "ZH" headings refer to codes for individual patients. Data are mean of technical triplicates ± SD (**p<.01, ***p<.001 one-way ANOVA followed by Tukey's post hoc test 95% CI).

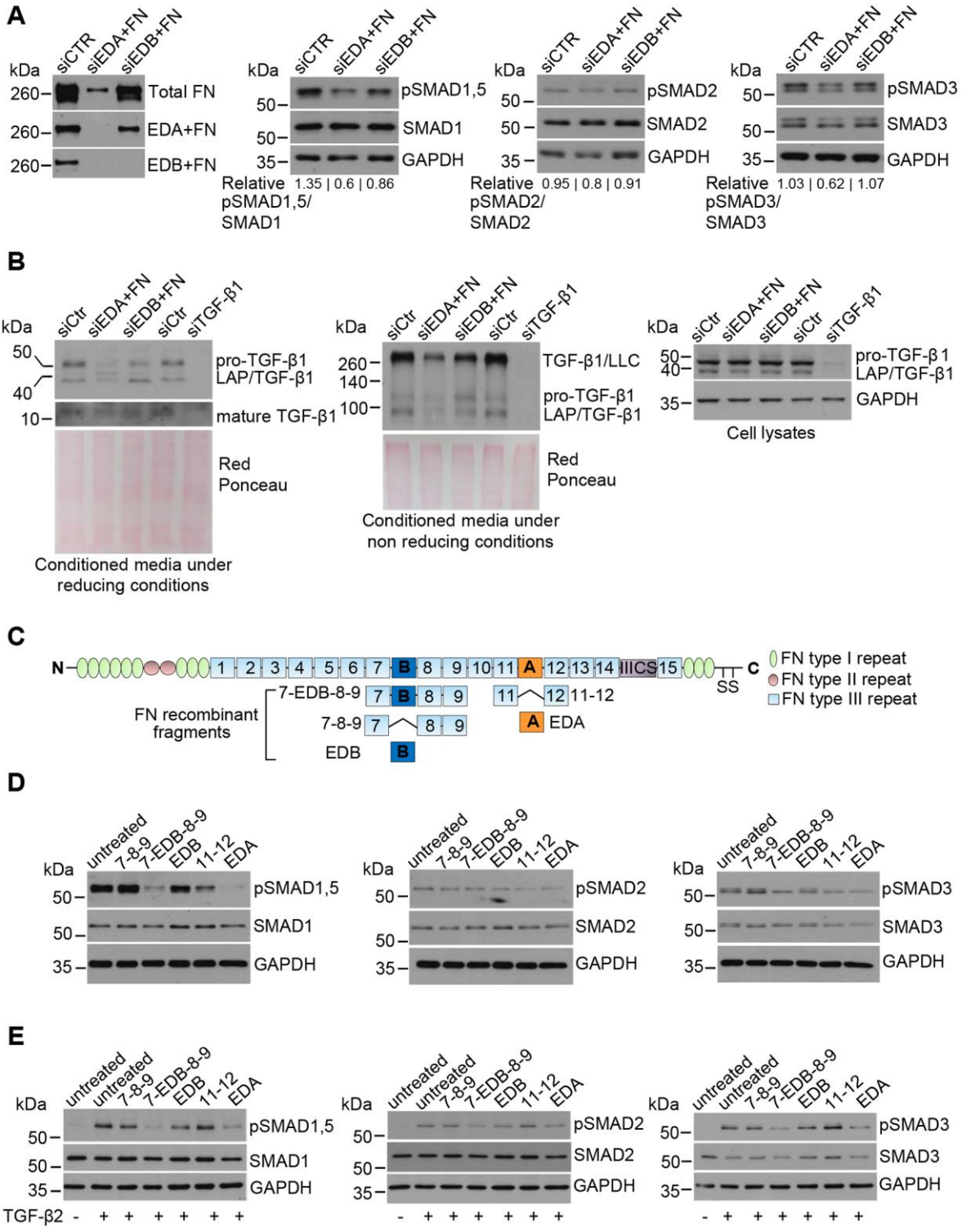

Figure 5. The EDA and EDB domains of fibronectin control TGF-β superfamily signaling in hCMEC. A. hCMEC were transfected with siRNA targeting the EDA or EDB domains of FN or non-targeting control siRNA (siCTR). At 24 h post transfection cells were transferred to a new dish and cultured in full medium. At 48 h post transfection cells were put in serum-free medium for 48 h. Concentrated conditioned culture media were analyzed for the levels of total FN, EDA+FN, and EDB+FN (left

panel). The levels of phosphorylated and total SMAD1,5, SMAD2 and SMAD3 were analyzed in cell lysates. The densitometry analysis of the immunoblot is indicated. **B.** The levels of pro-TGF-β1 (expected molecular weight of ~ 55 kDa), LAP/TGF-β1 (expected molecular weight of ~ 37 kDa), and mature TGF-β1 (expected molecular weight of ~ 12.5 kDa) were determined in the conditioned media of siCTR, siEDA+FN, siEDB+FN cells and in siTGF-β1 and the respective control cells under reducing conditions by immunoblot (left panel). The TGF-β1/large latent complex (~ 270 kDa), dimeric pro-TGF-β1 (~ 110 kDa) and dimeric LAP/TGF-β1 (~ 80 kDa) were detected in the same conditioned media analyzed under non-reducing conditions (central panel). Equal total protein loading was confirmed by red ponceau staining. Pro-TGF-β1, LAP/TGF-β1 and GAPDH were detected in the respective cell lysates analyzed under reducing conditions (right panel). **C.** Recombinant fragments of the FN molecule adjacent to the EDA and EDB domains including and excluding the extra-domains A and B used in this study. **D.** HCMEC were treated with the indicated FN recombinant fragments at 1 μM for 48 h. Levels of phosphorylated and total SMAD1,5, SMAD2 and SMAD3 were determined in cell lysates by immunoblot. **E.** HCMEC were treated with 1 μM FN recombinant fragments for 48 h and then exposed to 5 ng/ml TGF-β2 for 30 min. Levels of phosphorylated and total SMAD1,5, SMAD2 and SMAD3 were detected in cell lysates by immunoblot.

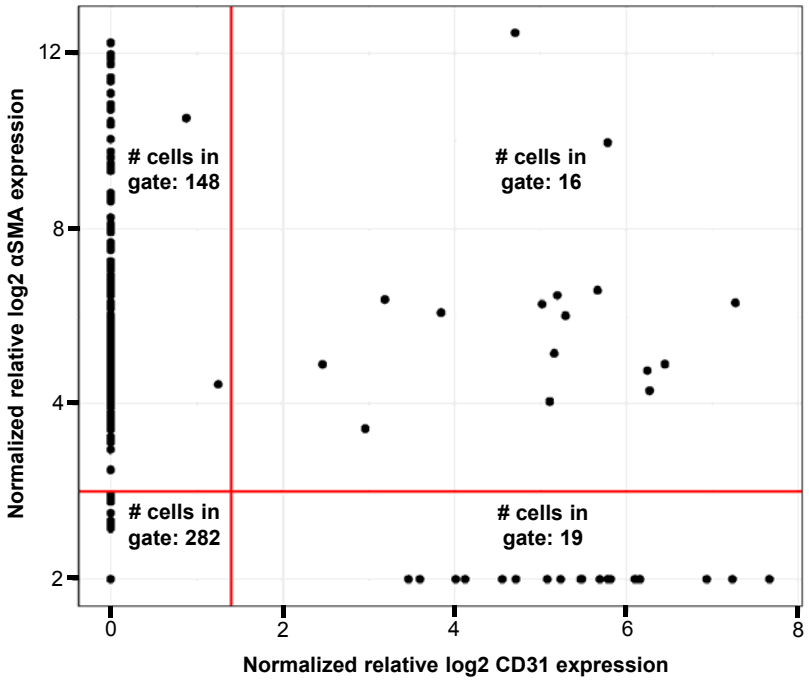

Fig. S1. Distribution of CD31 and αSMA expression in cells derived from freshly dissociated human glioblastoma. Single cell RT-PCR in cells derived from freshly dissociated human glioblastoma (N=6). X-axis: normalized relative log2 expression value of CD31, y-axis: normalized relative log2 expression value of αSMA.

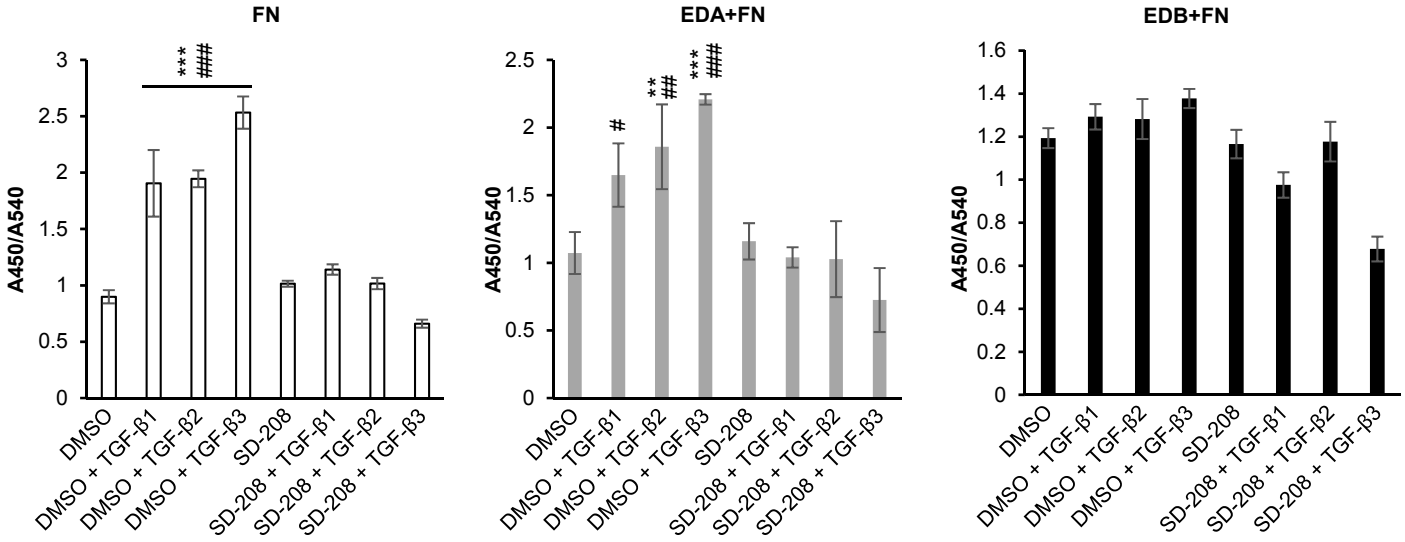

Fig. S2. Increased levels of insoluble total FN and EDA+FN in hCMEC treated with TGF-β1, TGF-β2 and TGF-β3. HCMEC were seeded at 2000 cells/well in 96-well plate. After 24 h cells were pre-incubated with 1 µM SD-208 or DMSO control for 1 h. Cells were then treated with 5 ng/ml TGF-β1, TGF-β2 or TGF-β3 for 72 h. Cells were then fixed and insoluble total FN, EDA+FN and EDB+FN were analyzed by ELISA. Another 96 well plate treated in the same manner was used for MTT assay 72 h post treatment. Data are expressed as the absorbance at 450 nm (ELISA assay) normalized by the absorbance at 540 nm (MTT assay). (* DMSO + TGF-β1 or TGF-β2 or TGF-β3 *vs.* DMSO; # DMSO + TGFβ1 or TGFβ2 or TGF-β3 *vs.* SD-208 + TGF-β1 or TGF-β2 or TGF-β3). Experiments were repeated three times. Data are mean of biological triplicates ± SD (*/#p<.05, **/##p<.01, ***/###p<.001 one-way ANOVA followed by Tukey's post hoc test 95% CI).

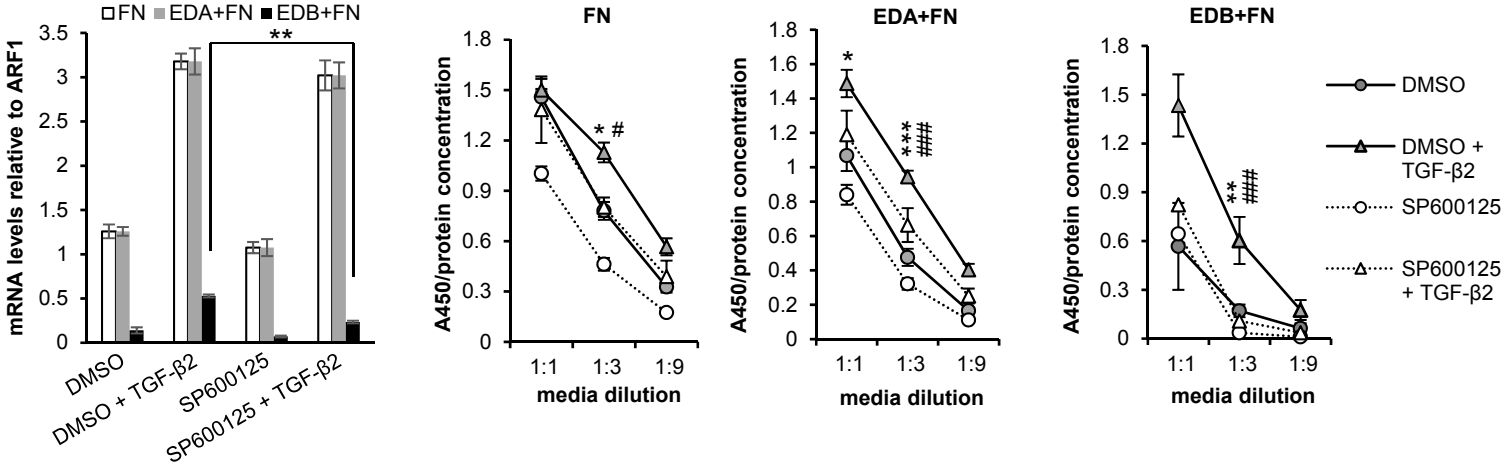

Fig. S3. JNK controls EDB+FN expression in hCMEC. FN, EDA+FN and EDB+FN mRNA (left panel) and protein levels (other panels) in hCMEC pre-incubated with 10 µM SP600125 for 2 h and then treated with 5 ng/ml TGF-β2 for 48 h (RNA data) or 72 h (protein data) (ELISA data: * DMSO + TGFβ2 *vs.* DMSO; # DMSO + TGFβ2 *vs.* SP600125 + TGFβ2). Media were tested at different dilutions and the data are shown as the values of absorbance at 450 nm divided by the protein concentration as measured in undiluted media (1:1). Data are mean of triplicates (technical for RT-PCR data and biological for ELISA data) ± SD (*/#p<.05, **/##p<.01, ***/###p<.001 one-way ANOVA followed by Tukey's post hoc test 95% CI).

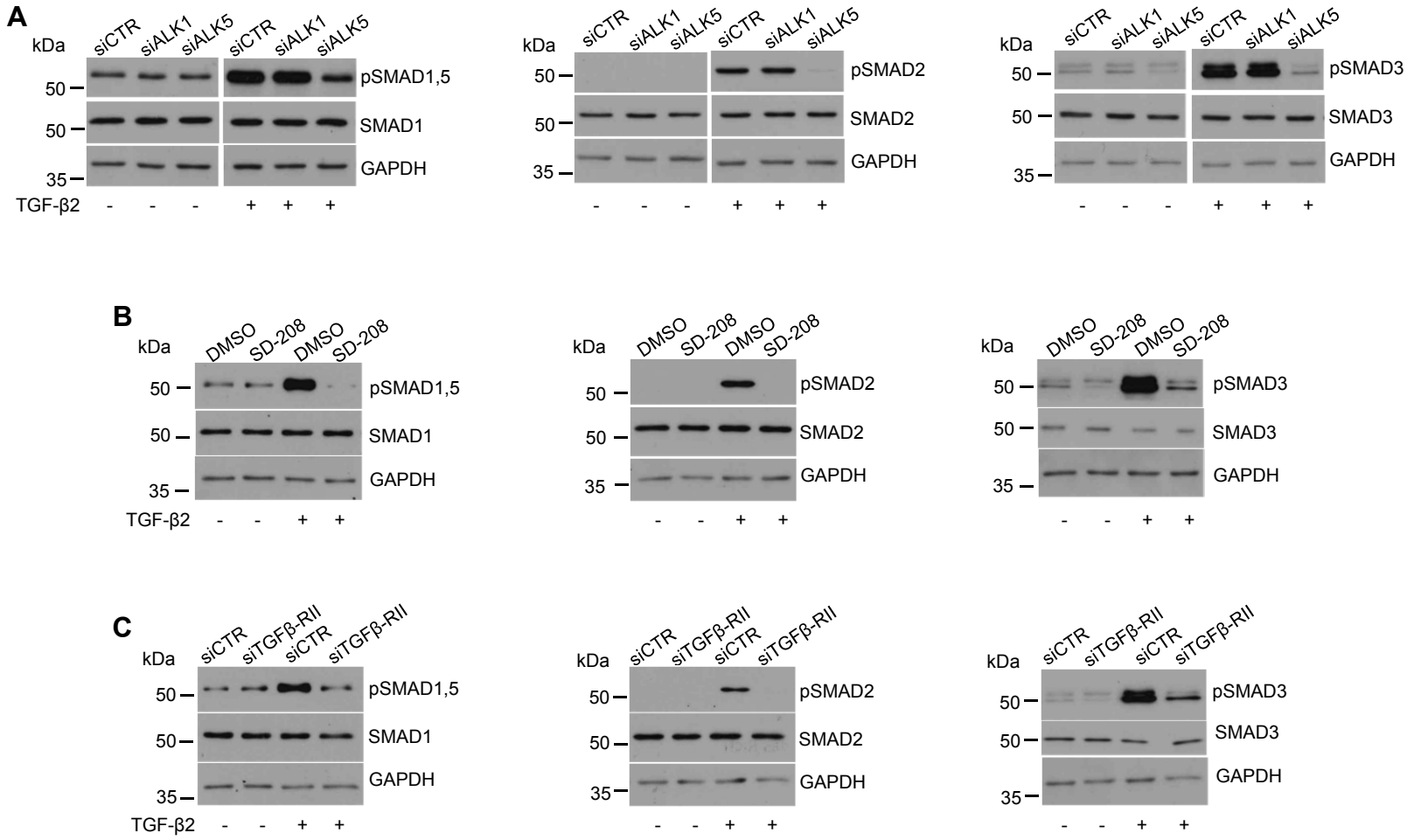

Fig. S4. TGF-β-induced SMAD phosphorylation is TGF-βRII- and ALK5-dependent in hCMEC. A. HCMEC were transfected with siCTR or siRNA targeting ALK1 or ALK5. At 24 h post transfection cells were placed in serum-free media for additional 24 h and then treated with 5 ng/ml TGF-β2 for 30 min. Total and phosphorylated SMAD were analyzed in cell lysates. **B.** HCMEC were serum starved for 24 h, pre-incubated with 1 µM SD-208 or DMSO as solvent control for 1 h and exposed to 5 ng/ml TGF-β2 for 30 min. **C**. HCMEC were transfected with siRNA targeting TGF-βRII or siCTR. At 24 h post-transfection cells were placed in serum-free media for additional 24 h and then treated with 5 ng/ml TGF-β2 for 30 min.

Primer name	Primer sequence
FN fwd	5'-TACACTGGGAACACTTACCG-3'
FN rev	5'-CCAATCTTGTAGGACTGACC-3’
EDA+FN fwd	5'-GGAGAGAGTCAGCCTCTGGTTCAG-3'
EDA+FN rev	5’-TCTGCAGTGTCTTCTTCACC-3’
EDB+FN fwd	5'-TCAAGGATGACAAGGAAAGTG-3'
EDB+FN rev	5'-AATAATGGTGGAAGAGTTTAGC-3'
SMAD2 fwd	5'-GCACTTGCTCTGAAATTTGGGC-3'
SMAD2 rev	5’-GACGACCATCAAGAGACCTGG-3’
SMAD3 fwd	5'-GCCTGTGCTGGAACATCATC-3'
SMAD3 rev	5'-TTGCCCTCATGTGTGCTCTT-3’
SMAD4 fwd	5'-GGTTCCTTCAAGCTGCCCTA-3'
SMAD4 rev	5'-ATGTGCAACCTTGCTCTCTCA-3’
TGF-β1 fwd	5'-GCCCTGGACACCAACTATTG-3’
TGF-β1 rev	5’-CGTGTCCAGGCTCCAAATG-3’
TGF-β2 fwd	5'-AAGCTTACACTGTCCCTGCTGC-3'
TGF-β2 rev	5'-TGTGGAGGTGCCATCAATACCT-3'
TGF-β3 fwd	5’-TCAGCCTCTCTCTGTCCACTT-3’
TGF-β3 rev	5’-CATCACCGTTGGCTCAGGG-3’
TGFBI fwd	5’-AAATCTGTGGCAAATCAACAGTCAT-3’
TGFBI rev	5’-TCCCAGGGTCTCGTAAAGGT-3’
LTBP1 fwd	5’-TACTTCATCCAAGACCGTTTTC-3’
LTBP1 rev	5’-AGGTCATCTTGGCCGTATCC-3’
LTBP2 fwd	5’-TTGACATAGACGAGTGCGCCA-3’
LTBP2 rev	5’-CACATACCGCCAGCATAAGCT-3’
LTBP3 fwd	5’-TTGTGAGGAGGTGGAGCAGC-3’
LTBP3 rev	5’-CGCAGAACACTGTGTCATCGA-3’
LTBP4 fwd	5’-AAGCTATGCTGGTTCCCTGG-3’
LTBP4 rev	5’-CGGCCTCATCACACTCGTTG-3’
CD31 fwd	5’-TTTGGACCAAGCAGAAGGCT-3’
CD31 rev	5’-TTGGCCGCAATGATCAAGAGA-3’
αSMA fwd	5’-GAGCGTGGCTATTCCTTCGTTA-3’
αSMA rev	5’-CCATCAGGCAACTCGTAACTCT-3’
ARF1 fwd	5'-GACCACGATCCTCTACAAGC-3'
ARF1 rev	5’-TCCCACACAGTGAAGCTG-3’

Table S1. Sequences of the primers used in the study.